

Coastal Flood Modelling of Ruawai, Kaihu-Dargaville and Awanui

Prepared for:



eCoast
eTakutai

**MOHIO - AUAHA - TAUTOKO
UNDERSTAND - INNOVATE - SUSTAIN**

PO Box 151, Raglan 3225, New Zealand
Ph: +64 7 825 0087 | info@ecoast.co.nz | www.ecoast.co.nz

Coastal Flood Modelling of Ruawai, Kaihu-Dargaville and Awanui

Report Status

Version	Date	Status	Approved by
V1	26/10/2017	Final Draft	STM
V2	30/10/2017	Rev.1	RM
V3	13/11/2017	Rev.2	RM
V4	21/11/2017	Rev.3	RM

It is the responsibility of the reader to verify the version number of this report.

Authors

Sam O'Neill <i>BSc, MSc (Hons)</i>
Rhys McIntosh <i>BSc, MSc (Hons)</i>
Jose Borrero <i>BSc, MSc, PhD</i>
Shaw Mead <i>BSc, MSc (Hons), PhD</i>

The information contained in this document, including the intellectual property, is confidential and propriety to Ecological and Physical Coastal Consultants Limited (T/A eCoast). It may be used by the persons to whom it is provided for the stated purpose for which it is provided, and must not be imparted to any third person without prior written approval from eCoast. eCoast reserves all legal rights and remedies in relation to any infringement of its right in respects of its confidential information. eCoast 2017

Executive Summary

eCoast Marine Consulting and Research was commissioned by Northland Regional Council to carry out a series of hydrodynamic flood simulations for Ruawai, Kaihu-Dargaville and Awanui. It was suspected that the previous 'bathtub' derived flood extents for various Coastal Flood Hazard Zone (CFHZ) areas were likely conservative and subsequent desktop analyses found that overtopping volumes could likely exceed bathtub volumes for future extreme events but may be less for current extreme events.

This assessment utilises CFHZ levels derived by Tonkin and Taylor (2016) to model extreme static water level scenarios that correspond to:

- CFHZ0 - 1% Annual Exceedance Probability (AEP) for 2015 water levels
- CFHZ1 - 2% AEP for 2065 water levels
- CFHZ2 - 1% AEP for 2115 water levels

These scenarios were used to derive storm surge boundary conditions for each of the model domains which contain high resolution LiDAR topography data, the best possible representations of flood defence structures, overland roughness parameterisation due to land cover type and background river flow rates. All model simulations have been undertaken using the HEC-RAS version 5.0 modelling suite (Hydraulic Engineering Centre – River Analysis System) developed by the U.S. Army Corps of Engineers.

Maximum flood extents calculated show less inundation when compared to previous studies undertaken by Barnett and MacMurray (2016) and Tonkin and Taylor (2016). This is mostly due to the implementation of spatially varying roughness in the HEC-RAS model runs, acting to represent the real resistance to flood flows that a rough surface type may have, such as mangroves or fernlands.

Contents

Executive Summary	i
Contents	ii
Figures.....	iii
Tables.....	iv
1 Introduction.....	1
1.1 Project Scope and Methodology	2
1.2 Previous Work and Literature Review	2
1.3 Datums and Coordinates	3
2 Model Set Up.....	4
2.1 Model Description	4
2.2 Preparation of Digital Terrain Models	4
2.3 Grid Development.....	9
2.4 Overland Roughness	10
2.5 Model Forcing and Boundary Conditions	11
2.5.1 Model Validation	12
2.5.2 CFHZ Boundary Conditions	14
3 Results.....	15
4 Study Limitations and Assumptions.....	18
5 Summary and Conclusions	19
6 References	20
Appendix A. Model Result Maps.....	21
Appendix B. CFHZ Boundary Conditions.....	37
Appendix C. waterRIDE.....	40

Figures

Figure 1.1. Location map for the study sites.....	1
Figure 2.1. Ruawai DTM. Red box indicates stopbank profile location for Figure 2.6.	5
Figure 2.2. Kaihu-Dargaville DTM. Red box indicates stopbank profile location for Figure 2.4.	5
Figure 2.3. Awanui DTM.	6
Figure 2.4. Kaihu-Dargaville DTM with pink line showing the location of the timber flood wall survey. Dargaville town is immediately landward of the stopbank.	6
Figure 2.5. LiDAR data plotted against surveyed data along the profile of the timber flood wall at Dargaville.....	7
Figure 2.6. Ruawai DTM with pink line showing the location of the stopbank survey. Ruawai town is immediately landward of the stopbank.	7
Figure 2.7. LiDAR data plotted against surveyed data for the stopbank at Ruawai.....	8
Figure 2.8. Gridded DTM of stopbanks overlain upon LiDAR at two locations along the Awanui River showing spatial inaccuracies (red circles) and general blockiness/staircasing.	9
Figure 2.9. Typical grid cell shapes at the 2D flow area boundaries (left) and grid cell arrangement enforced by break lines (left and right).	10
Figure 2.10. Land use types depicted for Ruawai with associated Manning's n values for varying roughness.....	11
Figure 2.11. Riverine and tidal boundary locations (red lines) for Ruawai (left), Kaihu- Dargaville (middle) and Awanui (right). In each domain, the longer of the two boundary locations represents the tidal boundary. Also shown are the extents of each of the model grids (shaded areas).....	13
Figure 2.12. Mean spring tidal conditions at Poutu Point (top) and Ben Gunn Wharf (bottom).	13
Figure 2.13. Mean spring water elevation conditions at Dargaville.	14
Figure 3.1. Comparison between combined Ruawai CFHZ2 flood extents (left) and Tonkin & Taylor (2016) bathtub model extents (right).....	15
Figure 3.2. Comparison between Kaihu-Dargaville CFHZ0 flood extents (left) and Barnett and MacMurray (2016) flood extents (right).	16
Figure 3.3. Comparison between Kaihu-Dargaville CFHZ1 flood extents (left) and Barnett and MacMurray (2016) flood extents (right).	16
Figure 3.4. Comparison between Kaihu-Dargaville CFHZ2 flood extents (left) and Tonkin and Taylor (2016) bathtub model extents (right).....	17
Figure 3.5. Comparison between Awanui CFHZ2 flood extents (left) and Tonkin and Taylor (2016) bathtub model extents (right).	17

Tables

Table 2.1. CFHZ levels for each site/cell (Tonkin and Taylor (2016)). 11

1 Introduction

eCoast Marine Consulting and Research was contracted by Northland Regional Council (NRC) to develop hydrodynamic flood models for low lying sites at Awanui, Kaihu-Dargaville and Ruawai (see Figure 1.1 for locations). This study follows on from the flood modelling undertaken by Tonkin and Taylor (2016) and Barnett and MacMurray (2016), which is discussed in Section 1.2. The objective of this study is to provide a more detailed and accurate flood risk assessment of three of Northland's most at-risk areas by using the HEC-RAS flood model with high resolution LiDAR topography data and comprehensive stopbank surveys. Three flood scenarios have been modelled:

- 1% Annual Exceedance Probability (AEP) 2015 static water level;
- the 2% AEP 2065 static water level, and;
- the 1% AEP 2115 static water level.

It is expected that these results will help inform NRC of the areas that will require stopbank upgrades or other flood aversion procedures.



Figure 1.1. Location map for the study sites.

1.1 Project Scope and Methodology

Low lying sites at Awanui, Dargaville-Wairoa and Ruawai are defended by coastal stopbanks. It was suspected that the bathtub-derived Coastal Flood Hazard Zone (CFHZ) areas were likely conservative. Subsequent simplified desktop analyses found that the overtopping volumes likely exceed the bathtub volumes for future extreme levels, but may be underestimated for current extreme levels. Hydrodynamic modelling would account for a fluctuating tidal time series, variation in stopbank heights and overland roughness which would slow inundation. Furthermore, hydrodynamic modelling could be undertaken to better understand the coastal flood extents for lower, more frequent flood levels (i.e. 10-year annual recurrence interval) and to provide information on flood depths/velocities to inform damage assessments and assist in prioritising stop bank upgrades.

The following methodology has been applied to this project:

- a) Set up a HEC-RAS flood model Digital Terrain Model (DTM) using existing LiDAR data provided by NRC.
- b) Extract existing stopbank elevations from the DTM or from data provided by NRC and use this information to modify the computational domain as required.
- c) Define the roughness based on assumed terrain and best-practice guidelines.
- d) Derive single time series boundary conditions based on nearby recorded tidal series adjusted to CFHZ0, CFHZ1, CFHZ2 elevations. The length of the timeseries will depend on typical storm tide duration for that site.
- e) Sensitivity tests for model domain size, repeating steps a to c until optimal grid cell size is determined.
- f) Run three inundation scenarios for each model domain and output shapefiles for maximum flow depth, maximum water surface elevation and maximum velocity.
- g) Produce preliminary report for review.
- h) Update modelling based on review.
- i) Finalise model output maps and report.

1.2 Previous Work and Literature Review

Previous reports related to this work include:

- Tonkin and Taylor (2016) Coastal Flood Hazard Zones for Select Northland Sites, and;
- Barnett and MacMurray Ltd. (2016) Coastal Flood Hazard Zone Modelling for Kaihu Valley, Dargaville and Awakino Floodplain.

Tonkin and Taylor (2016) assessed and mapped CFHZs around the Northland region considering astronomical tides, storm surge, medium-term fluctuations in sea level, wave processes and long-term changes in mean sea level. Extreme static and dynamic levels were presented corresponding to the extent of the 1% Annual Exceedance Probability (AEP) 2015 static water level (CFHZ0), the 2% AEP 2065 static water level (CFHZ1), the 1% AEP 2115 static water level (CFHZ2) and the 1% AEP 2115 dynamic water level (CRHZ), where dynamic refers to the process of wave run-up.

A connected bathtub model was used to map flood extents meaning that areas flooded only if they were naturally hydraulically connected to the coastal water body or via a structure such as a drainage channel or culvert. The coastal run-up hazard zones were mapped by applying an attenuation model to the maximum run-up elevations. Calculated run-up levels were validated using run-up debris measurements deposited after a storm event in January 2008.

Barnett and MacMurray (2016) modelled CFHZs for Dargaville, Kaihu valley and Awakino floodplain. These simulations were conducted using Tonkin and Taylor's (2016) CFHZ0, CFHZ1 and CFHZ2 levels applied to a tidal time series measured in September 2005 at the Dargaville river gauge when the largest high tide event was recorded since the beginning of the 35-year record. In other words, the September 2005 time series was adjusted to match each of the CFHZ levels.

Modelling was conducted with the TUFLOW 2D model of the Dargaville, Awakino and Kaihu floodplains, and a Mike 11 model of the Kaihu valley up to Kaihu Gorge. The models were connected via a transfer of boundary conditions and the output was joined. This study assumed low flows in all rivers and accounted for all existing flood defence features in the model domain.

1.3 Datums and Coordinates

All elevations (levels) presented in this report are presented in terms of One Tree Point Vertical Datum 1964 (OTP64). Mean sea level varies with respect to OTP64 around the Northland coast resulting in slightly different inundation levels, even where exposure is similar.

The coordinate reference system used for this project is New Zealand Transverse Mercator (NZTM).

2 Model Set Up

2.1 Model Description

For the hydrodynamic modelling, the HEC-RAS 5.0 modelling suite (Hydraulic Engineering Centre – River Analysis System) developed by the U.S. Army Corps of Engineers as part of the “Next Generation” of hydraulic engineering software was applied. In addition to the river analysis system, the model encompasses rainfall-runoff analysis (HEC-HMS), reservoir system simulation (HEC-ResSim), flood damage analysis (HEC-FDA and HEC-FIA) and real-time river forecasting for reservoir operations (CWMS).

HEC-RAS is capable of simulating two-dimensional unsteady flow through a full network of open channels, alluvial fans and floodplains and can perform subcritical, supercritical and mixed flow regime calculations. The basic computational procedure solves the full-dynamic two-dimensional Saint Venant equations (2D shallow water equations) using an implicit finite difference method. Further detail about the model can be found in the HEC-RAS 5.0 User’s Manual.

2.2 Preparation of Digital Terrain Models

DTMs, shown in Figure 2.1, Figure 2.2 and Figure 2.3, were created based on topographic data from several sources. High resolution 2 m x 2 m LiDAR topography data was supplied by the NRC, while additional topographic data was sourced from Land Information New Zealand (LINZ). Bathymetry data in the northern Kaipara Harbour was taken from hydrographic charts provided by LINZ.

Stopbank crest elevations were extracted from LiDAR data, although the crest of the stopbank and timber flood wall at Dargaville CBD has also been surveyed (see Figure 2.4 for location). Figure 2.5 illustrates the difference in timber flood wall elevations represented in the two data sets, and clearly shows that the LiDAR does not resolve the elevations sufficiently, therefore, the surveyed data was incorporated in to the model terrain. The reason that the LiDAR poorly represents flood wall elevations in this location is due to the structure itself being quite narrow therefore cannot be resolved in a 2 m x 2 m grid.

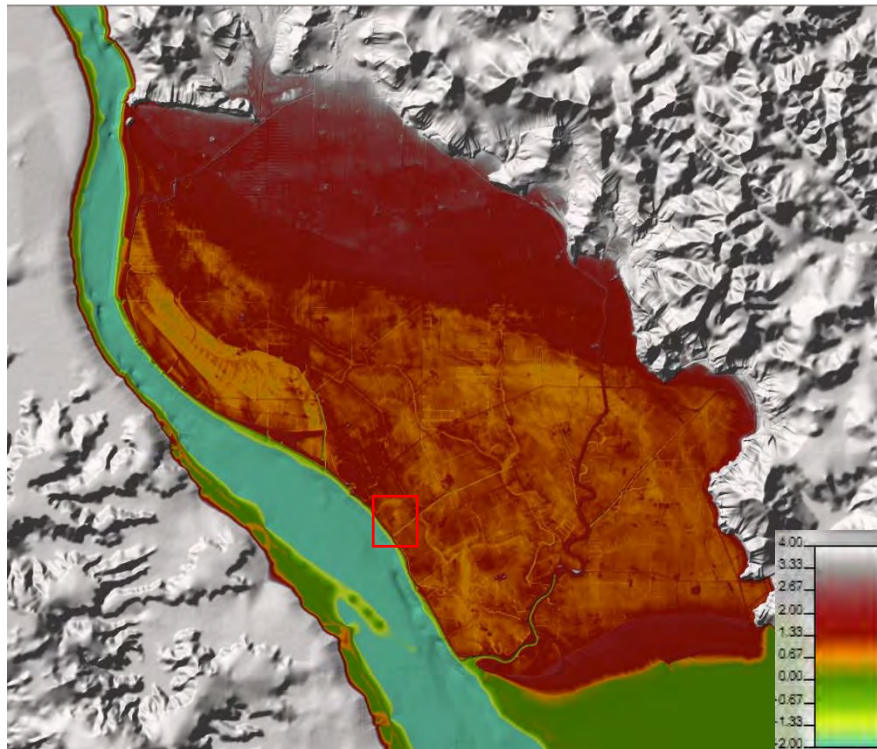


Figure 2.1. Ruawai DTM. Red box indicates stopbank profile location for Figure 2.6.

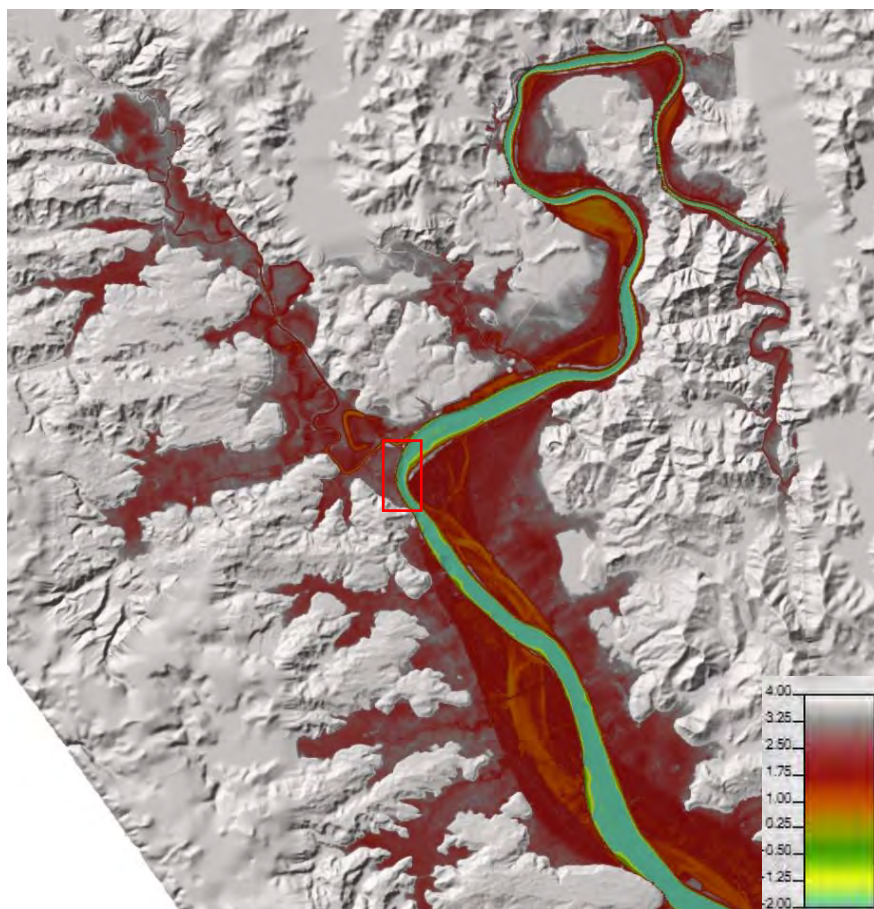


Figure 2.2. Kaihu-Dargaville DTM. Red box indicates stopbank profile location for Figure 2.4.

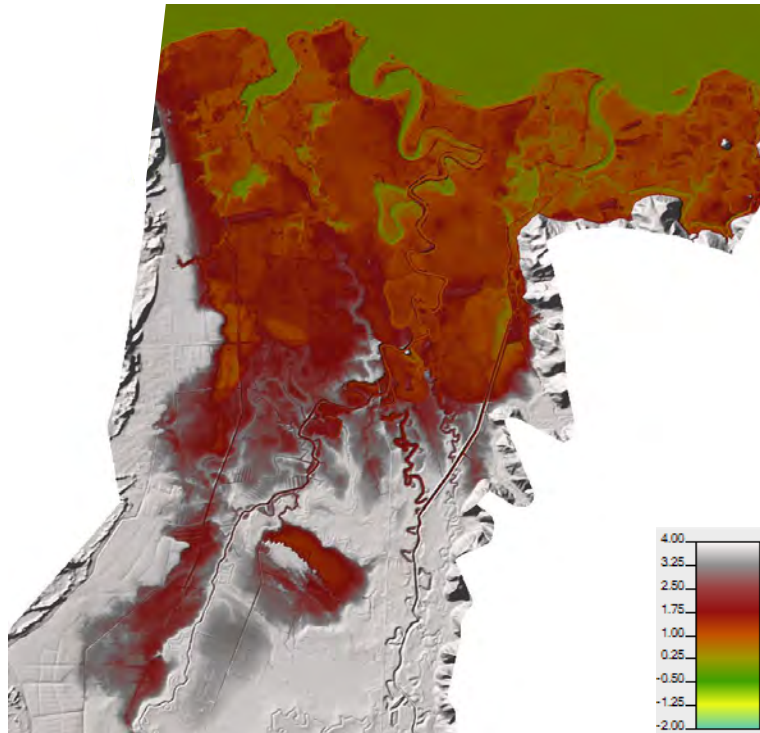


Figure 2.3. Awanui DTM.



Figure 2.4. Kaihu-Dargaville DTM with pink line showing the location of the timber flood wall survey. Dargaville town is immediately landward of the stopbank.

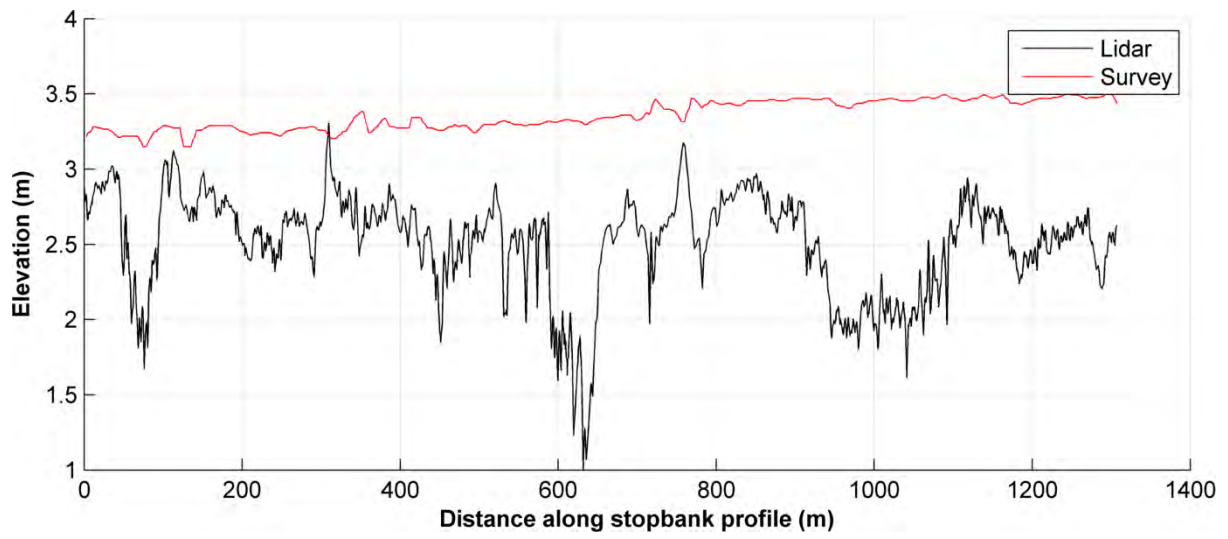


Figure 2.5. LIDAR data plotted against surveyed data along the profile of the timber flood wall at Dargaville.



Figure 2.6. Ruawai DTM with pink line showing the location of the stopbank survey. Ruawai town is immediately landward of the stopbank.

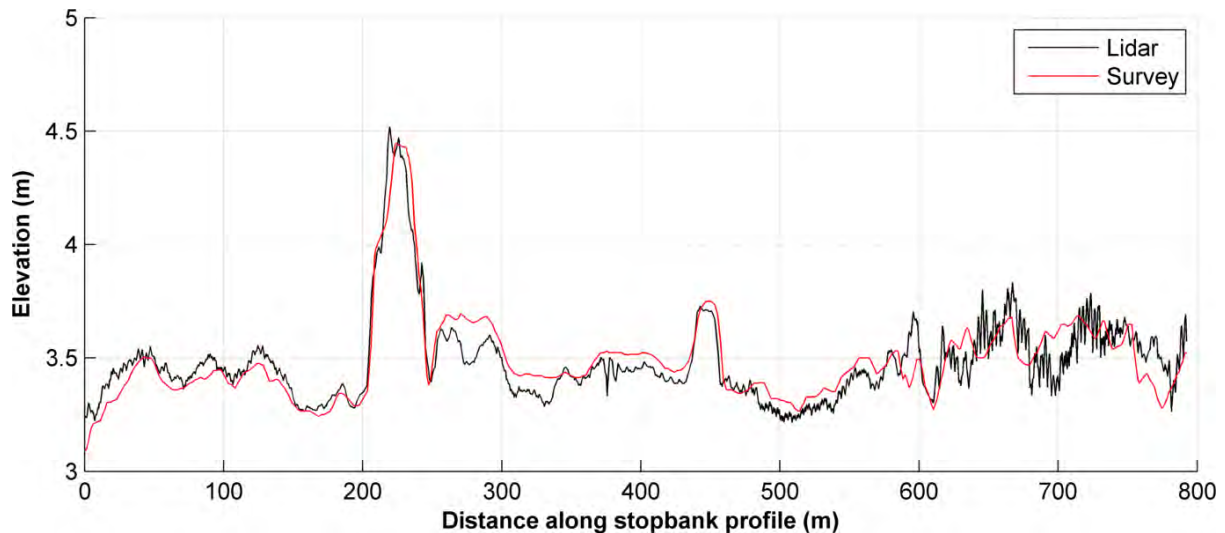


Figure 2.7. LiDAR data plotted against surveyed data for the stopbank at Ruawai.

Ruawai stopbank data (see Figure 2.6 for location) was treated in a similar way to Dargaville as can be seen in Figure 2.7, although in this case, the LiDAR does extremely well in representing actual stopbank crest elevations, since this feature is an earth mound several meters wide. The surveyed data for this location was therefore not incorporated into the model terrain. The only manipulations made to the Ruawai DTM were in five locations where the LiDAR did not sufficiently resolve floodgate elevations. These elevations were provided by NRC and were incorporated into the model domain as stopbanks rather than one-way flow structures as drainage was not relevant to the model scenarios.

For the Awanui estuary, surveyed stopbank crest levels were provided in a gridded DTM and as point data. This survey was the most extensive and covered the majority of the banks of the multiple-channel system within the northern part of the Awanui DTM (Figure 2.3). Unfortunately, the gridded DTM of the stopbank elevations, illustrated in Figure 2.8, proved to be too blocky and spatially inaccurate. Average water levels would breach the stopbanks at the apex of the 'staircase' features in preliminary model runs. Additionally, the point data supplied had relatively large gaps of more than 10 m between survey points along the stopbank crests in some areas, and so gridding and incorporating these data into the model terrain posed some difficulty. LiDAR stopbank elevations at Awanui however, were checked against the surveyed data and were deemed to be mostly accurate with some small spots requiring manual editing to better represent actual crest elevations. A good model validation was achieved with this approach.



Figure 2.8. Gridded DTM of stopbanks overlain upon LiDAR at two locations along the Awanui River showing spatial inaccuracies (red circles) and general blockiness/staircasing.

Good bathymetry data for the Rangaunu estuary is unavailable and so a flat platform was introduced set to 0 m in elevation to represent the intertidal region (Figure 2.3). It is important to note that with the introduction of spatially varying roughness, which is discussed in Section 2.4, flow is naturally constrained to the estuarine channels over this 0 m intertidal flat since the roughness coefficient for open channels is set to 0.03, a value which is much lower than that for mangroves (0.3).

2.3 Grid Development

Model grids, or 2D flow areas, were constructed for each of the three domains encompassing all open channels, alluvial fans, floodplains and other flood pathways. The initial cell size was set to 15 m x 15 m resulting in a mostly rectilinear mesh, with the exception of the cells adjacent to the grid boundaries that take an irregular shape in order to ‘snap’ to the shape of the 2D flow area. An example of this is illustrated in Figure 2.9.

Any feature acting as a barrier to flow identified in each of the model terrains such as stopbanks, raised roads, river and creek banks, canal banks, drainage ditch banks etc., required break lines to be enforced into the grid. This means that such features received greater cell resolution on each of their sides as well as forcing cell faces along their crest lengths (Figure 2.9). The smallest grid cells created as a result of this procedure were 2 m x 2 m, matching the LiDAR resolution of the underlying terrain.

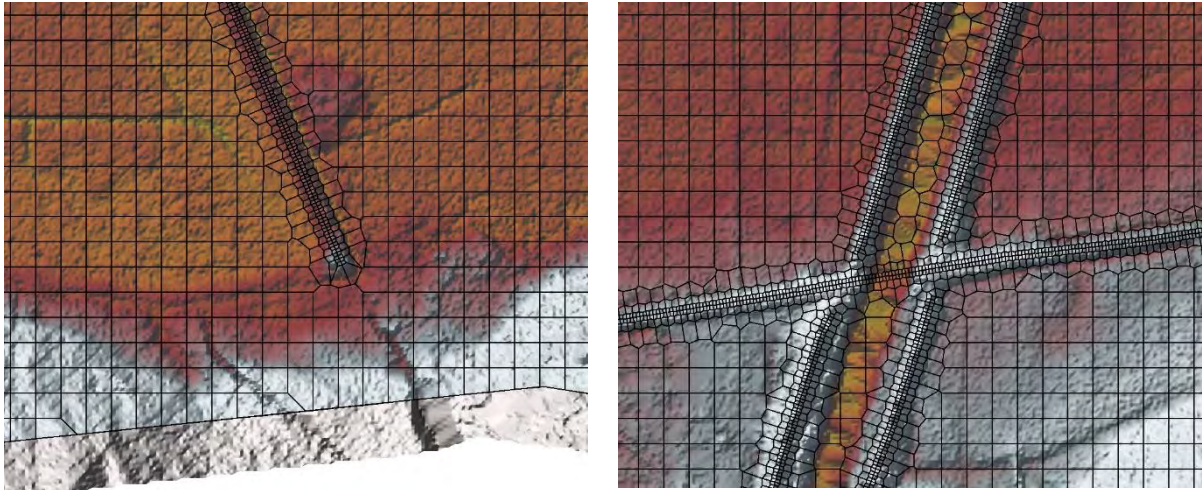


Figure 2.9. Typical grid cell shapes at the 2D flow area boundaries (left) and grid cell arrangement enforced by break lines (left and right).

2.4 Overland Roughness

HEC-RAS has the capability of defining spatially variable roughness within the model domain. This allows for realistic representation of the resistance to flood flows over rough land cover such as fernlands or mangroves. This was done by assigning Manning's roughness coefficients (Manning's n values) to each land use type recognised in the region. Land use shape files for each of the three model domains were acquired from the Land Resource Information Systems (LRIS) data portal and Manning's n values were assigned following U.S. Geological Survey Water Resources Division (1984) and Chow (1959). Figure 2.10 presents the Manning's n values used along with an example of the spatial distribution of the different land uses at Ruawai. It is also important to note that in regions where a land use was not specified, a default Manning's n value of 0.06 was applied to all model runs.

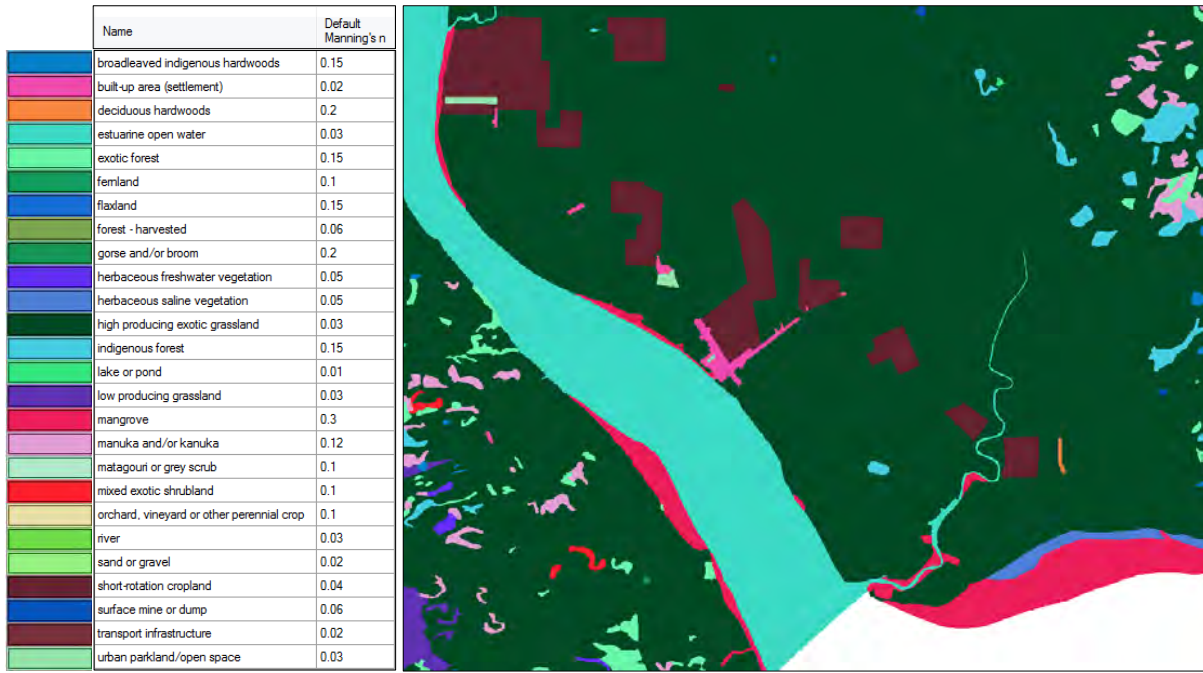


Figure 2.10. Land use types depicted for Ruawai with associated Manning's n values for varying roughness.

2.5 Model Forcing and Boundary Conditions

CFHZ levels derived by Tonkin and Taylor (2016) which consist of storm tide (assessed from site data), wave set up and sea-level rise, have been assessed as follows: For each site/cell, and event tabulated, a tidal time series has been derived with maxima consistent with the CFHZ values in Table 2.1 below and applied as boundary conditions to force the model. That is, CFHZ0, CFHZ1 and CFHZ2 represent storm surge levels corresponding to the current 1% Annual Exceedance Probability (AEP), 2% AEP with 2065 sea-level rise and 1% AEP with 2115 sea-level rise respectively.

Table 2.1. CFHZ levels for each site/cell (Tonkin and Taylor (2016)).

Name	No.	Name	Type	Cell	Type	MHS	Current 1% AEP (m OTP)			2065 2% AEP (m OTP)			2115 1% AEP (m OTP)				
							Storm tide	CFHZ0	CFHZ1	Storm tide	CFHZ0	CFHZ1	Storm tide	CFHZ0	CFHZ1		
Awanui estuary	44	Awanui estuary	Estuary		Estuary	1.08	1.76	2.10	2.08	1.76	2.20	2.3	2.1	2.8	3.0	2.8	3.0
Kaihu estuary	57	Kaihu estuary	Estuary		Estuary	1.68	2.81	2.96	2.68	2.81	3.29	3.3	3.2	3.8	3.9	3.8	3.9
Dargaville - Wairoa	58	Dargaville - Wairoa	Estuary		Estuary	1.72	2.84	2.97	2.72	2.84	3.29	3.3	3.2	3.8	3.9	3.8	3.9
Ruawai	59	Ruawai	Estuary	A	Estuary	1.71	2.92	3.13	2.71	2.92	3.33	3.7	3.3	3.9	4.3	3.9	4.3
				B	Estuary	1.71	3.02	3.27	2.71	3.02	3.32	3.5	3.4	4.0	4.2	4.0	4.2

The Kaihu-Dargaville model runs, however, were treated in a slightly different way since the tide gauge data that Tonkin and Taylor (2016) used to derive CFHZ levels there, is located on the river bank in the town centre of Dargaville, i.e. right in the middle of the model domain. Unlike Ruawai and Awanui, which have measured tidal records (and derived CFHZ levels)

relatively close to their tidal boundary locations, Kaihu-Dargaville required additional tidal input at the downstream boundary location to raise the water surface elevations at the tide gauge location to the appropriate CFHZ levels. This is discussed in Section 2.5.2.

2.5.1 Model Validation

In order to validate each of the three models, mean spring tidal and riverine conditions were used to force the model for a duration of 24-hours allowing for two tidal cycles and beginning at the bottom of low tide. The results of these validation runs were checked to ensure that no stopbank breaches or artificial flooding was occurring as well as ensuring that river channels and tributaries filled to appropriate background levels. See Appendix A for the mapped validation results. All boundary forcing locations are shown in Figure 2.11.

The tidal signals used for these routines (northern Kaipara and Rangaunu Harbours) are shown in Figure 2.12 and show a mean spring tidal amplitude of 1.55 m in the northern Kaipara and 1.15 m in the Rangaunu Harbour. Tidal data was acquired from the Poutu Point gauge in Kaipara Harbour for the Kaihu-Dargaville and Ruawai model runs, and the Ben Gunn Wharf gauge in the Rangaunu Harbour for the Awanui model runs.

Riverine flow for all Ruawai model runs was applied to the Wairoa River according to mean spring water elevation conditions measured at Dargaville. The Wairoa River water elevation at this location is tidally dominated and it was determined that the mean spring tide peak elevation for the data record was 2.15 m (see Figure 2.13). In order to ensure that the phase difference between the river and the tidal boundary forcing was appropriate, the Wairoa River record was shifted accordingly to reflect the delay observed as the tidal wave propagates up the river.

For the Kaihu-Dargaville model runs, the upper Wairoa River boundary was forced with a constant stage of 1.5 m as this location was deemed to be beyond the tidal zone. With a lack of water surface elevation data upstream of Dargaville, this value was derived from historical aerial photographs and extrapolated from the LiDAR riverbank elevations. Additionally, a constant flow of 1 m³/s was applied to the Awakino River and a constant flow of 6 m³/s to the Kaihu River, as per Barnett and MacMurray (2016).



Figure 2.11. Riverine and tidal boundary locations (red lines) for Ruawai (left), Kaihu-Dargaville (middle) and Awanui (right). In each domain, the longer of the two boundary locations represents the tidal boundary. Also shown are the extents of each of the model grids (shaded areas).

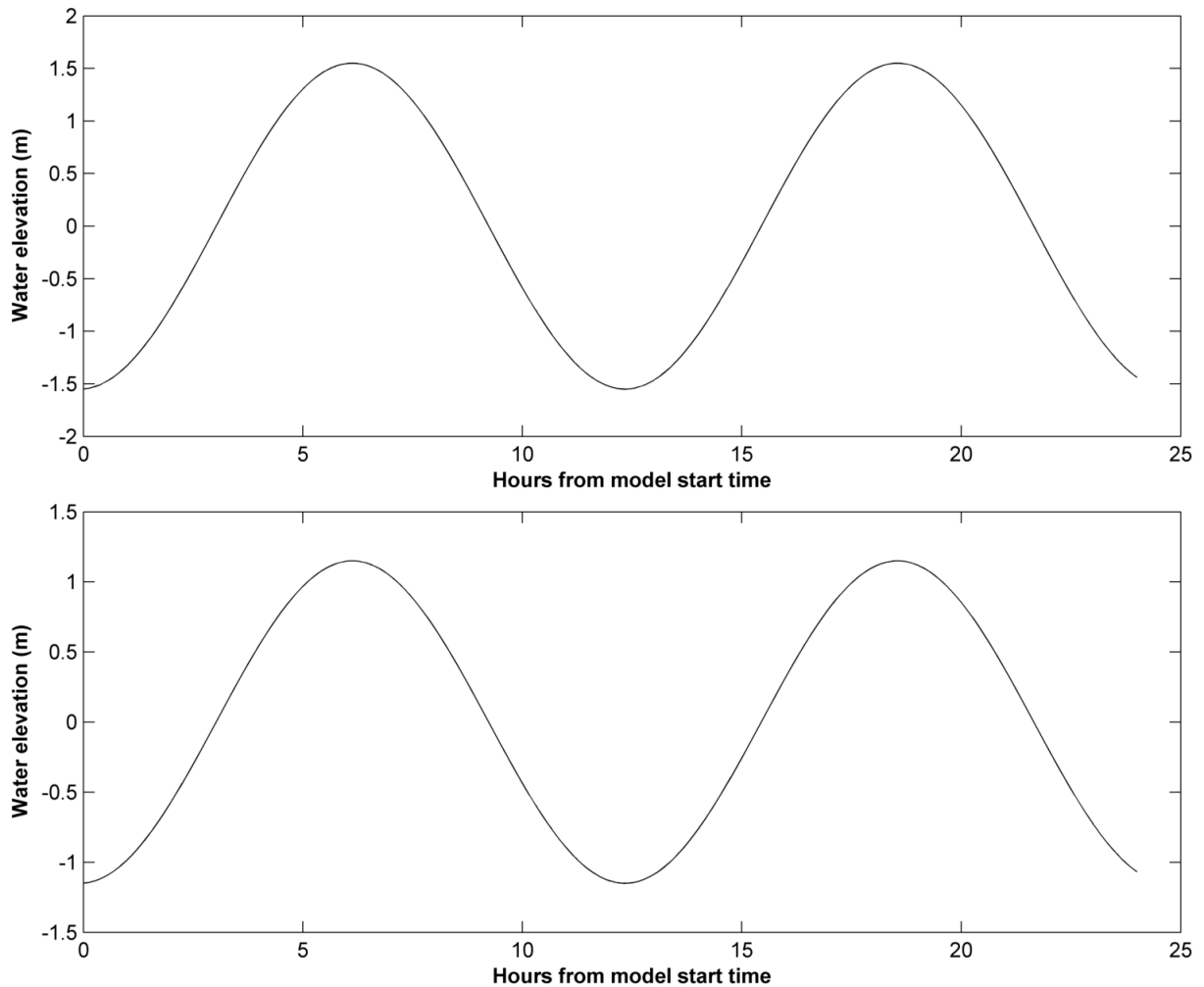


Figure 2.12. Mean spring tidal conditions at Poutu Point (top) and Ben Gunn Wharf (bottom).

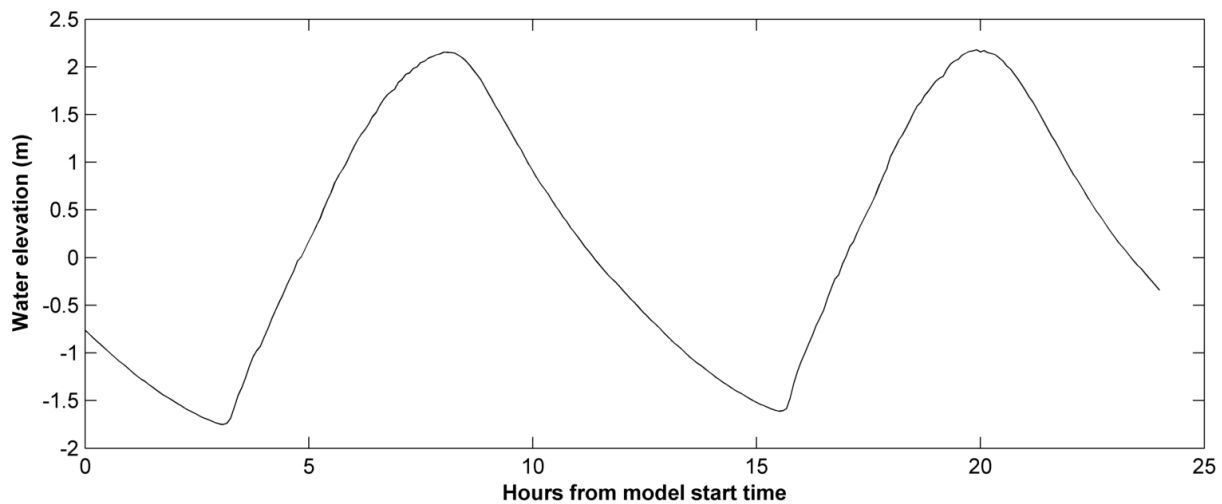


Figure 2.13. Mean spring water elevation conditions at Dargaville.

2.5.2 CFHZ Boundary Conditions

For the CFHZ0, CFHZ1 and CFHZ2 model runs, a simple approach has been taken to construct appropriate tidal boundary conditions for each scenario. This involved taking a 24-hour mean spring tidal curve from either Poutu Point (Ruawai and Kaihu-Dargaville model runs) or Ben Gunn Wharf (Awanui model runs), as displayed in Figure 2.12, and manipulating the second high-tide peak to correspond to the CFHZ level. For the CFHZ1 and CFHZ2 cases in all model domains, sea-level rise coefficients as reported by Tonkin and Taylor (2016) were applied to the leading tidal wave. This amounted to an upward shift of 0.4 m and 1.0 m respectively. In the case of Kaihu-Dargaville, the entire lower boundary time series was further raised by a factor of 0.4 m for all scenarios as this was the adjustment required to achieve the desired CFHZ0 level at Dargaville (Table 2.1), to be consistent with the 1% AEP river level assessed from the site record.

This approach was deemed to yield time series that represent a real storm surge scenario the best when compared to typical storm surge measurements. All CFHZ boundary condition plots can be seen in Appendix B. Furthermore, unlike Barnett and MacMurray (2016) who employed a model duration of 62-hours, a 24-hour model duration has been selected since drainage structures such as culverts and other small underpasses are not represented in the HEC-RAS model domains. Inevitably, storm surge flood models that do not represent drainage structures accurately show increased flood extent error with increased model durations, as water is unrealistically unable to drain away after each high tide during the storm surge event.

3 Results

All model results were processed into raster files of maximum water surface elevation, maximum water velocity and maximum depth. These can be seen in Appendix A. Several flood extent polygons provided by Barnett and MacMurray (2016) and Tonkin and Taylor (2016) are available for viewing on the NRC GIS map viewer. These have been compared to the HEC-RAS flood extent output shape files in Figure 3.1, Figure 3.2, Figure 3.3, Figure 3.4 and Figure 3.5.

It can be seen for the CFHZ2 results at Ruawai (Figure 3.1), that the flood extents are substantially less than the bathtub results. This can be mostly attributed to the effect that overland roughness has on floodwater propagation over land. There are a few regions where mangroves significantly slow inundation, most notably the large stand immediately to the south of the Ruawai floodplain but also just to the north of Ruawai township.

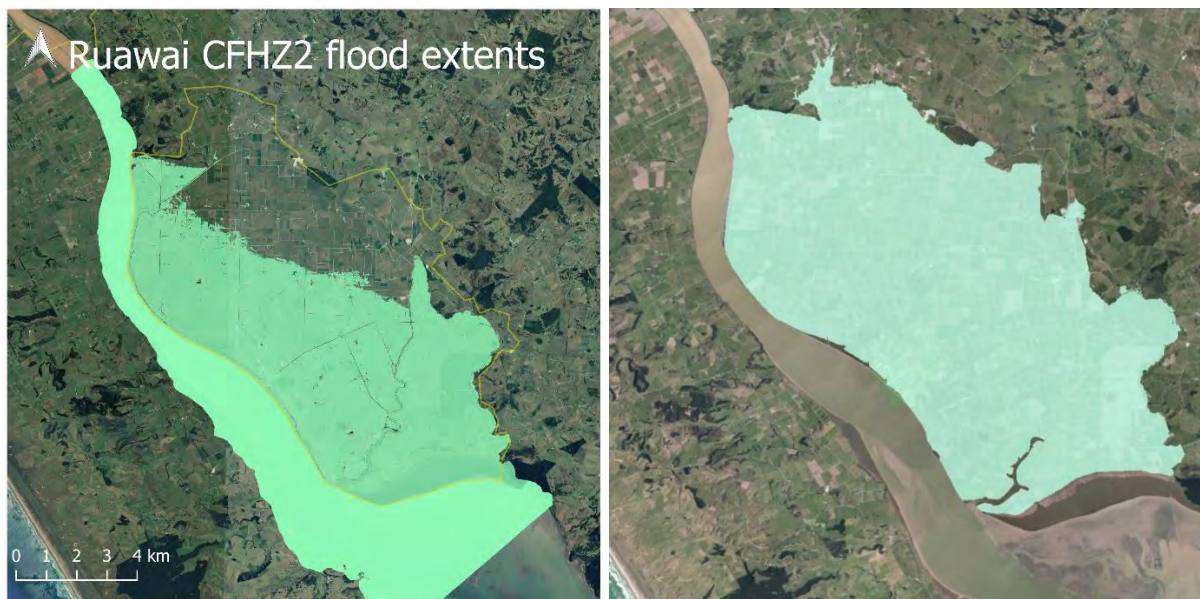


Figure 3.1. Comparison between combined Ruawai CFHZ2 flood extents (left) and Tonkin & Taylor (2016) bathtub model extents (right).

CFHZ0 and CFHZ1 flood extents at Kaihu-Dargaville (Figure 3.2 and Figure 3.3 respectively) are somewhat reduced for the west bank of the Wairoa when compared with those from the Barnett and MacMurray (2016) study. Again, this is predominantly a consequence of overland roughness. The east bank was not modelled by Barnett and MacMurray (2016), however, substantial flooding is observed in the HEC-RAS results for the low-lying region across the river from Dargaville township.

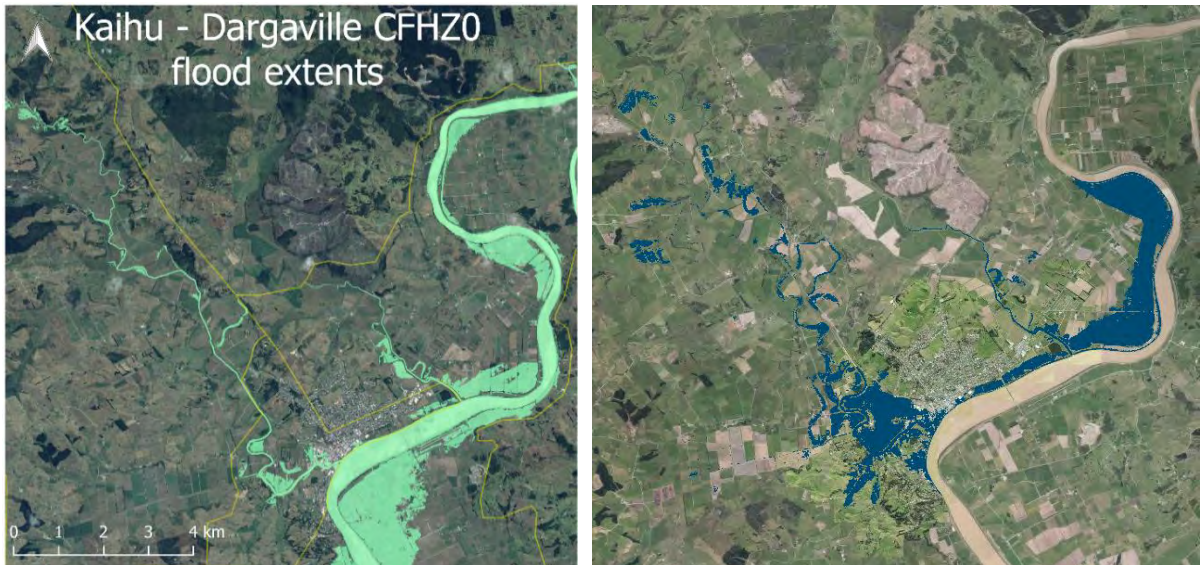


Figure 3.2. Comparison between Kaihu-Dargaville CFHZ0 flood extents (left) and Barnett and MacMurray (2016) flood extents (right).

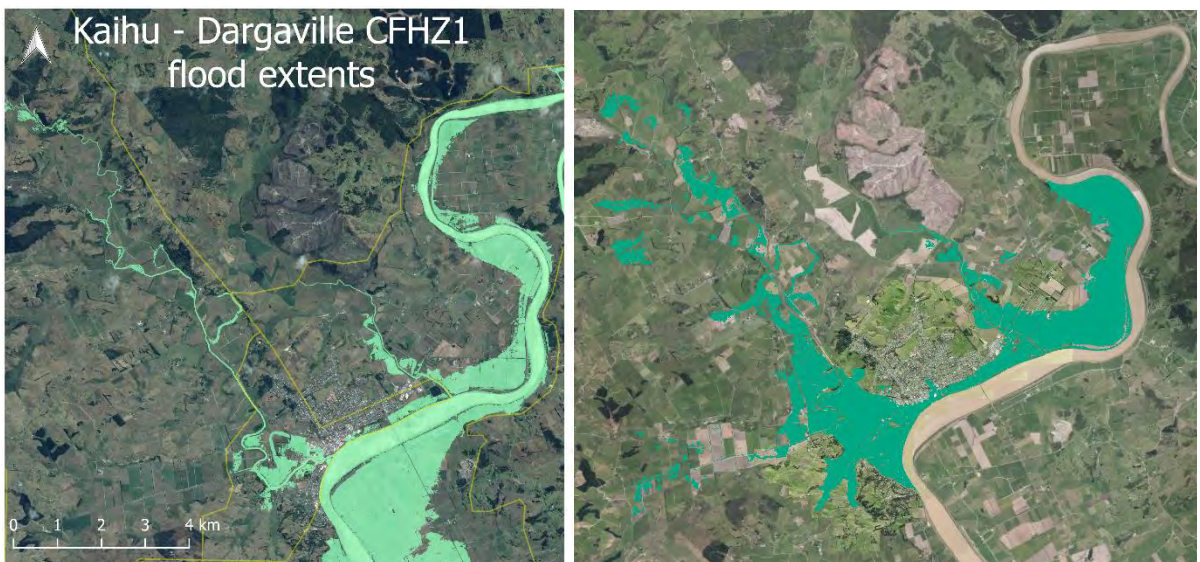


Figure 3.3. Comparison between Kaihu-Dargaville CFHZ1 flood extents (left) and Barnett and MacMurray (2016) flood extents (right).

The CFHZ2 flood extents at Kaihu-Dargaville when compared to the bathtub results from Tonkin and Taylor (2016), as seen in Figure 3.4, show a similar pattern to one another. This is likely a result of the lower portion of the model domain becoming saturated (floodplains completely inundated) and therefore allowing higher water surface elevations to flow upstream of Dargaville, ultimately reaching near-bathtub levels. In addition, the bathtub results show inundation in the Manganui River which the HEC-RAS results do not. This is due to the fact that riverine flow data was unavailable and therefore was not introduced to this tributary for this study.

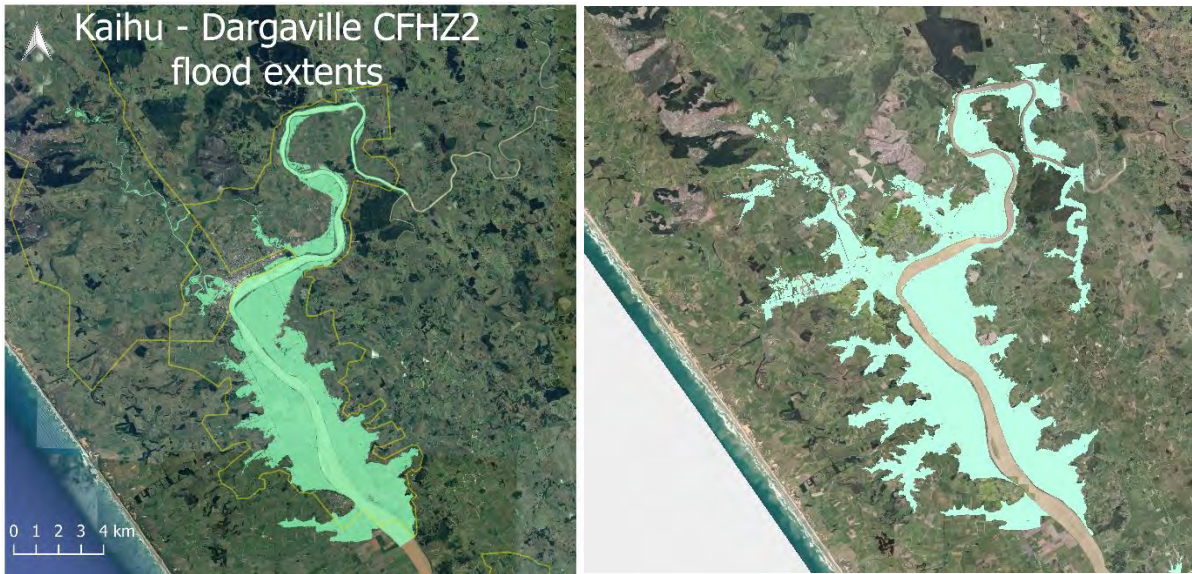


Figure 3.4. Comparison between Kaihu-Dargaville CFHZ2 flood extents (left) and Tonkin and Taylor (2016) bathtub model extents (right).

Flood extent results at Awanui, as expected, fall short of the bathtub limits. Again, this is due to the effect of overland roughness, particularly in the large regions of mangroves present in the Rangaunu estuary.

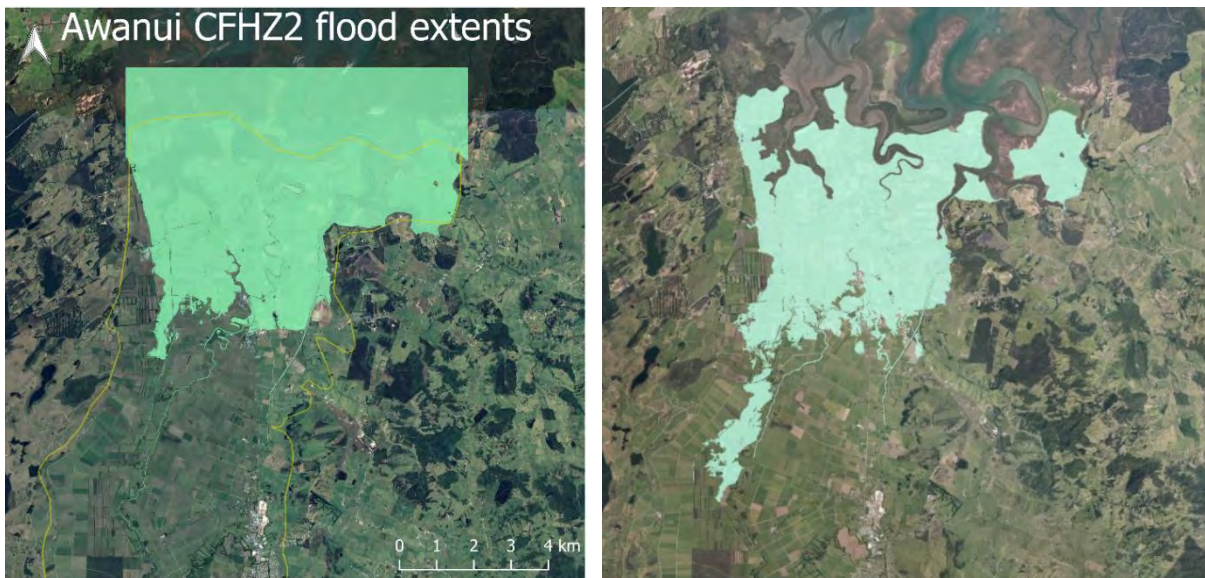


Figure 3.5. Comparison between Awanui CFHZ2 flood extents (left) and Tonkin and Taylor (2016) bathtub model extents (right).

4 Study Limitations and Assumptions

- 1) Bathymetry data for Kaipara Harbour and the Wairoa River was taken from Hydrographic Chart 4265 which yielded reasonable depths, however greater model accuracy could be achieved with up-to-date surveyed channel data, in the Kaipara Harbour, the Wairoa River and the Rangaunu Harbour.
- 2) Storm rainfall was not considered in this study and can have a significant influence on storm surge flood extents.
- 3) Boundary condition locations were chosen to maximise model accuracy based on available tide and terrain/bathymetry data, however, greater accuracy could be achieved if either:
 - a) Tidal records were available at Ruawai, or
 - b) Good terrain/bathymetry data were available linking Poutu Point to the Manganui/Wairoa junction. This would allow for a combined Ruawai-Kaihu-Dargaville model domain that would more accurately predict storm surge conditions at the Dargaville tide gauge.
- 4) Water surface elevation/flow data upstream of Dargaville is not available. This freshwater input into the Kaihu-Dargaville system has a bearing on storm surge results there and was only able to be estimated for this study.
- 5) Manganui River flow was not implemented in any of the Kaihu-Dargaville model runs as data was unavailable. The additional contribution of freshwater and the ability for a 'full' river to facilitate storm surge flooding could be considered for greater model accuracy.
- 6) Drainage structures were not represented in the HEC-RAS model domains. These features can alter the flow of floodwaters both onto and away from low-lying regions.

5 Summary and Conclusions

- 1) Hydrodynamic models (HEC-RAS version 5.0) of Ruawai, Kaihu-Dargaville and Awanui were used to simulate coastal flooding under three extreme scenarios:
 - a. CFHZ0 - 1% AEP for 2015 water levels
 - b. CFHZ1 - 2% AEP for 2065 water levels
 - c. CFHZ2 - 1% AEP for 2115 water levels
- 2) The models were validated using mean spring tidal and riverine flow conditions for a period of 24-hours, ensuring that no flooding was occurring and typical water levels were observed.
- 3) The maximum flood extents calculated show less inundation when compared to two previous studies undertaken by Barnett and MacMurray (2016) and Tonkin and Taylor (2016). This is mostly due to the implementation of spatially varying roughness in the HEC-RAS model runs, acting to represent the real resistance to flood flows that a rough surface type may have, such as mangroves or fernlands.
- 4) Maximum water surface elevation, maximum water velocity and maximum depth shape files of coastal flood extents have been supplied to NRC.

6 References

- Barnett and MacMurray Ltd. (2016). Coastal Flood Hazard Zone Modelling for Kaihu Valley, Dargaville and Awakino Floodplain. Technical Report prepared for Northland Regional Council, May 2016.
- Chow, V.T., (1959). Open-Channel Hydraulics: New York, McGraw-Hill, 680 p.
- HEC-RAS (2016). U.S. Army Corps of Engineers Institute for Water Resources Hydraulic Engineering Centre River Analysis System – User’s Manual Version 5.0
- Tonkin and Taylor Ltd. (2016). Coastal Flood Hazard Zones for Select Northland Sites. Technical Report prepared for Northland Regional Council, May 2016.
- U.S. Geological Survey Water Resources Division (1984). Guide for Selecting Manning’s Roughness Coefficients for Natural Channels and Floodplains. Technical Report number FHWA-TS-84-204.

Appendix A. Model Result Maps

Ruawai validation

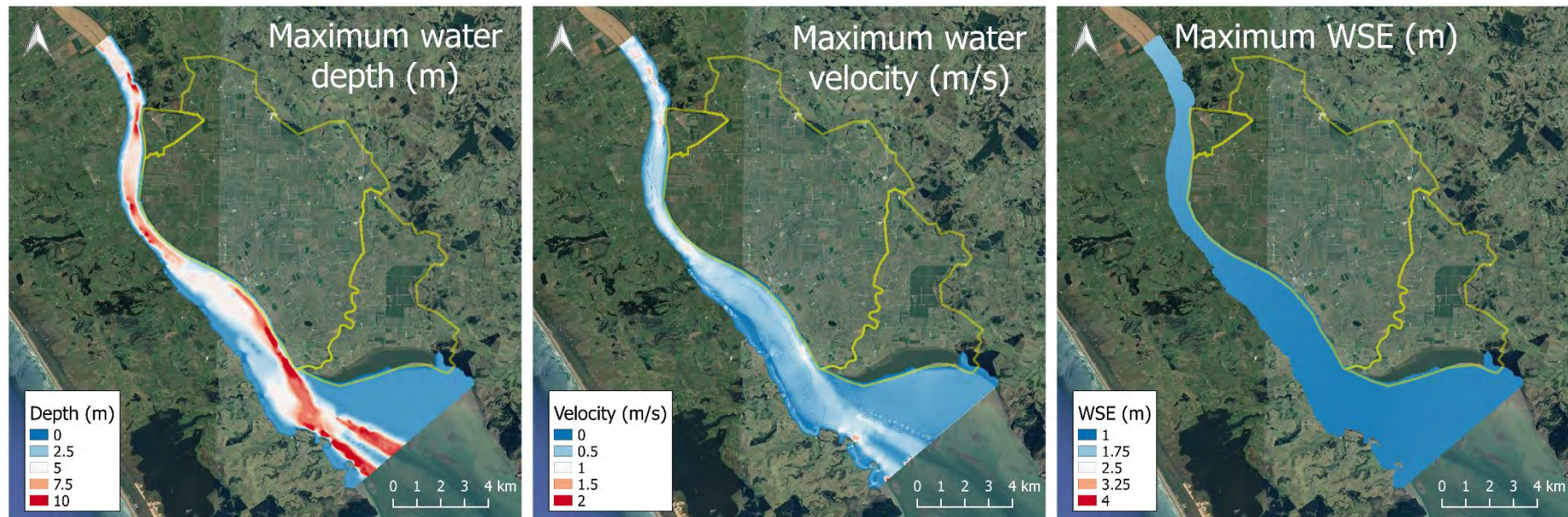


Figure 6. Ruawai validation model run maximum depth, velocity and water surface elevation. Yellow line shows hazard assessment zones.

Ruawai cell A CFHZ0

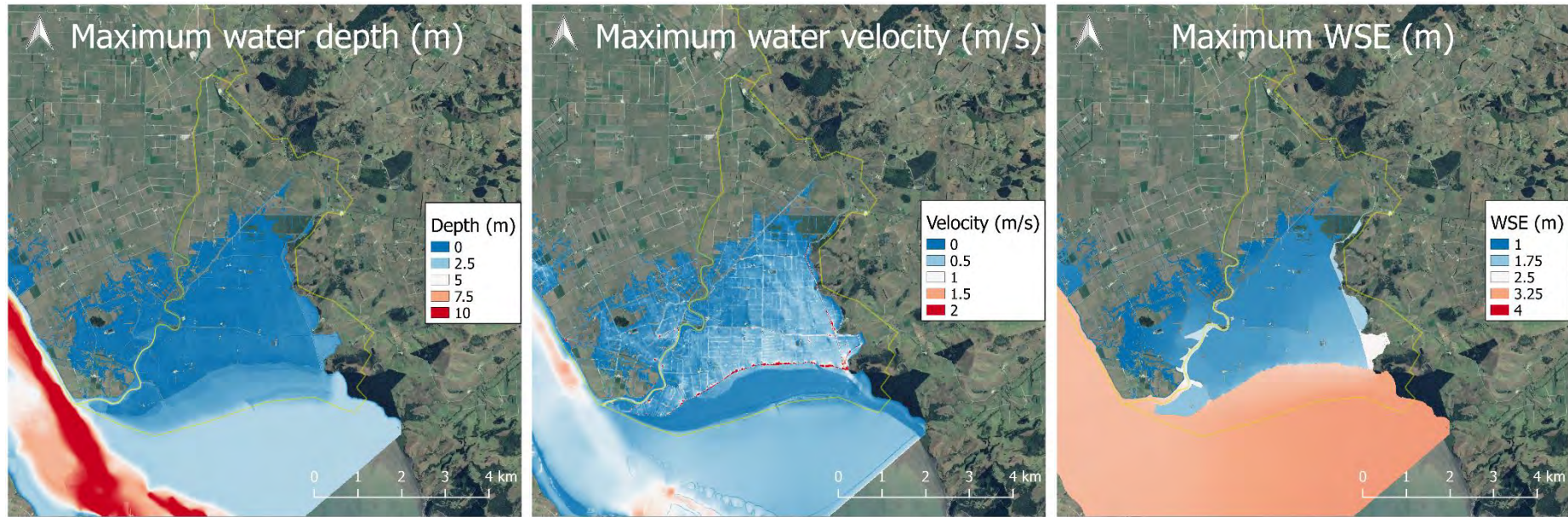


Figure 7. Ruawai cell A CFHZ0 model run maximum depth, velocity and water surface elevation. Yellow line shows hazard assessment zones.

Ruawai cell A CFHZ1

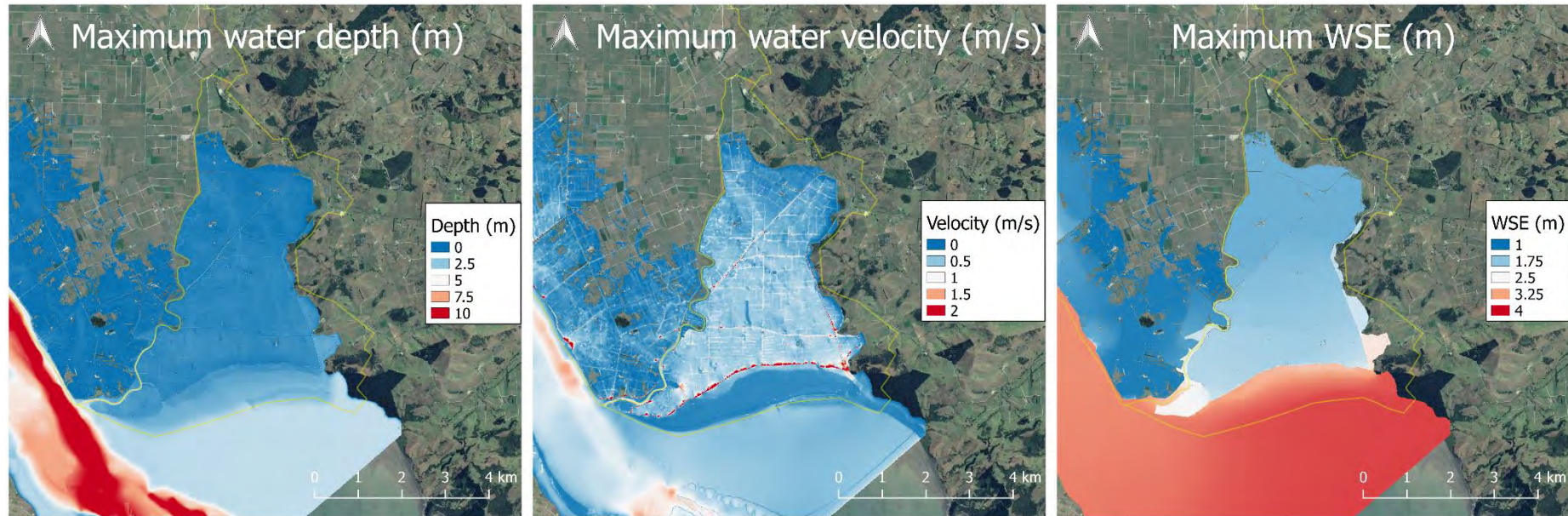


Figure 8. Ruawai cell A CFHZ1 model run maximum depth, velocity and water surface elevation. Yellow line shows hazard assessment zones.

Ruawai cell A CFHZ2

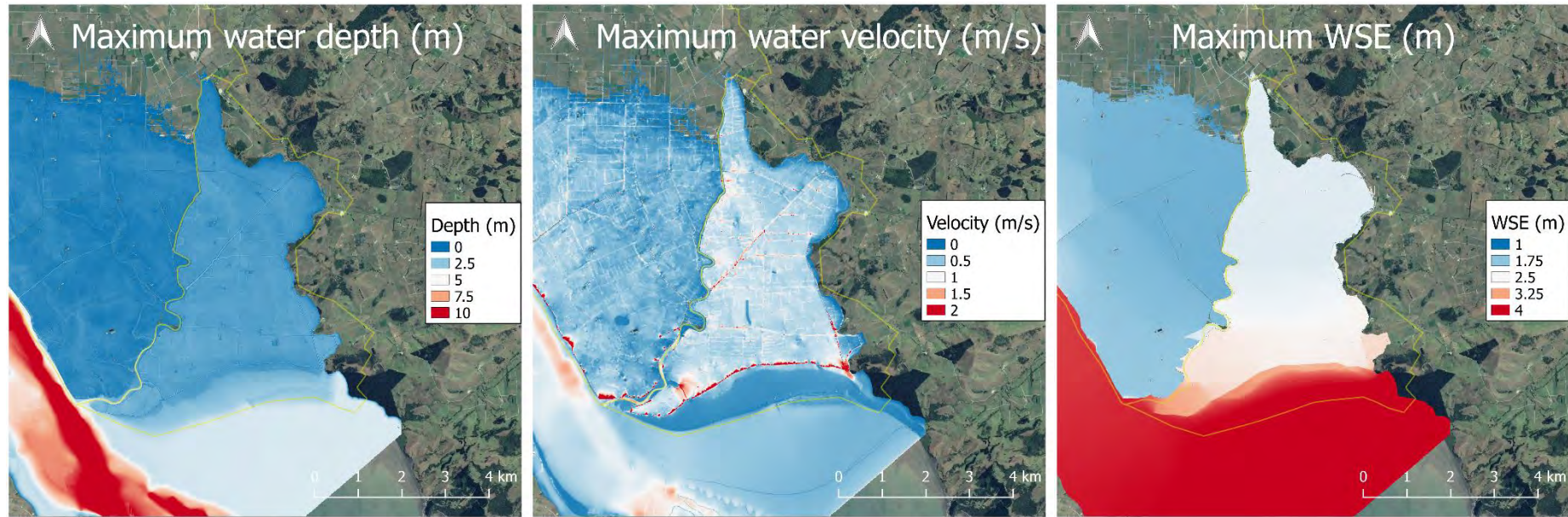


Figure 9. Ruawai cell A CFHZ2 model run maximum depth, velocity and water surface elevation. Yellow line shows hazard assessment zones.

Ruawai cell B CFHZ0

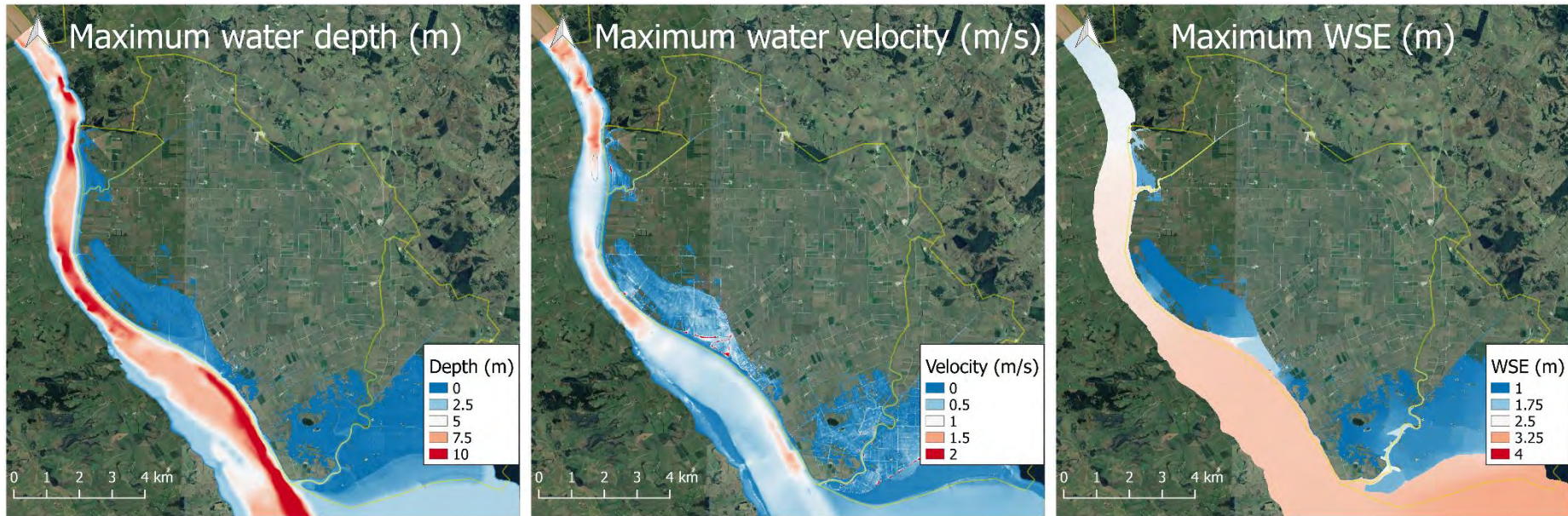


Figure 10. Ruawai cell B CFHZ0 model run maximum depth, velocity and water surface elevation. Yellow line shows hazard assessment zones.

Ruawai cell B CFHZ1

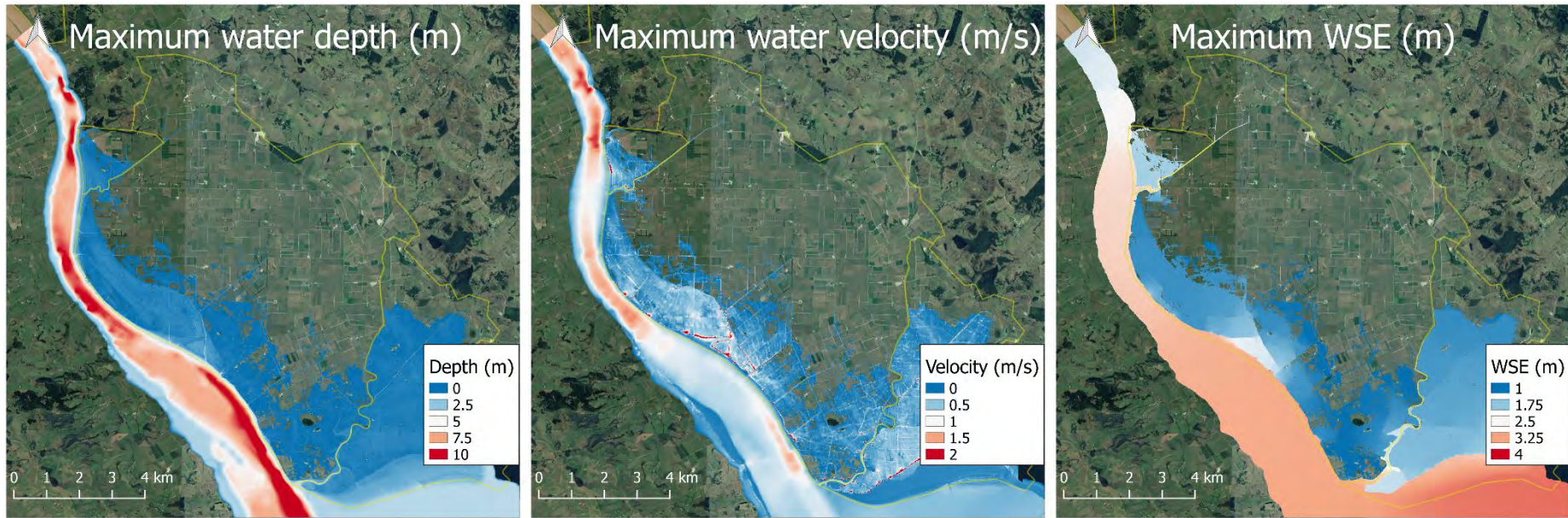


Figure 11. Ruawai cell B CFHZ1 model run maximum depth, velocity and water surface elevation. Yellow line shows hazard assessment zones.

Ruawai cell B CFHZ2

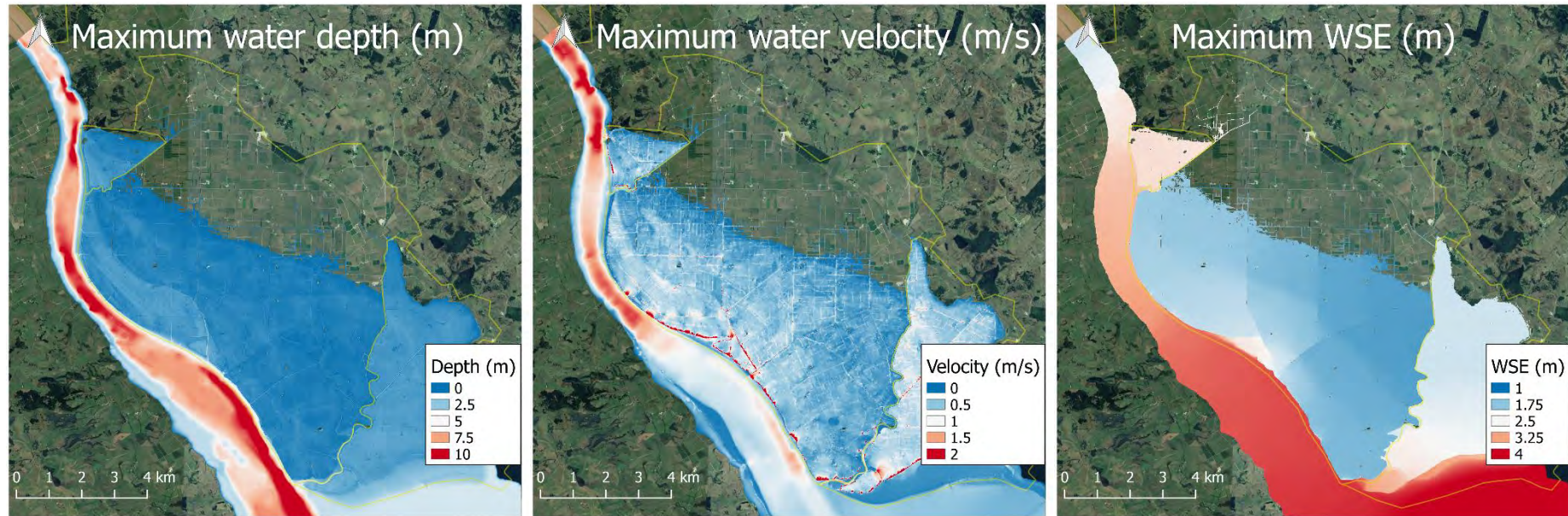


Figure 12. Ruawai cell B CFHZ2 model run maximum depth, velocity and water surface elevation. Yellow line shows hazard assessment zones.

Kaihu – Dargaville validation

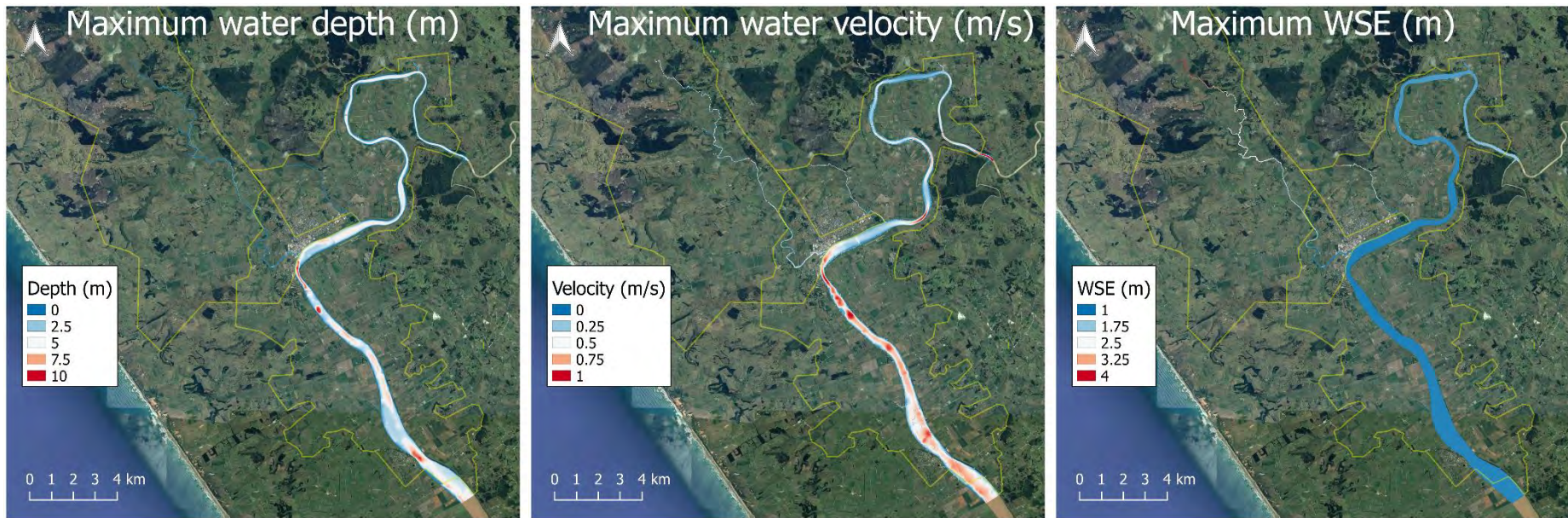


Figure 13. Kaihu – Dargaville validation model run maximum depth, velocity and water surface elevation. Yellow line shows hazard assessment zones.

Kaihu – Dargaville CFHZ0

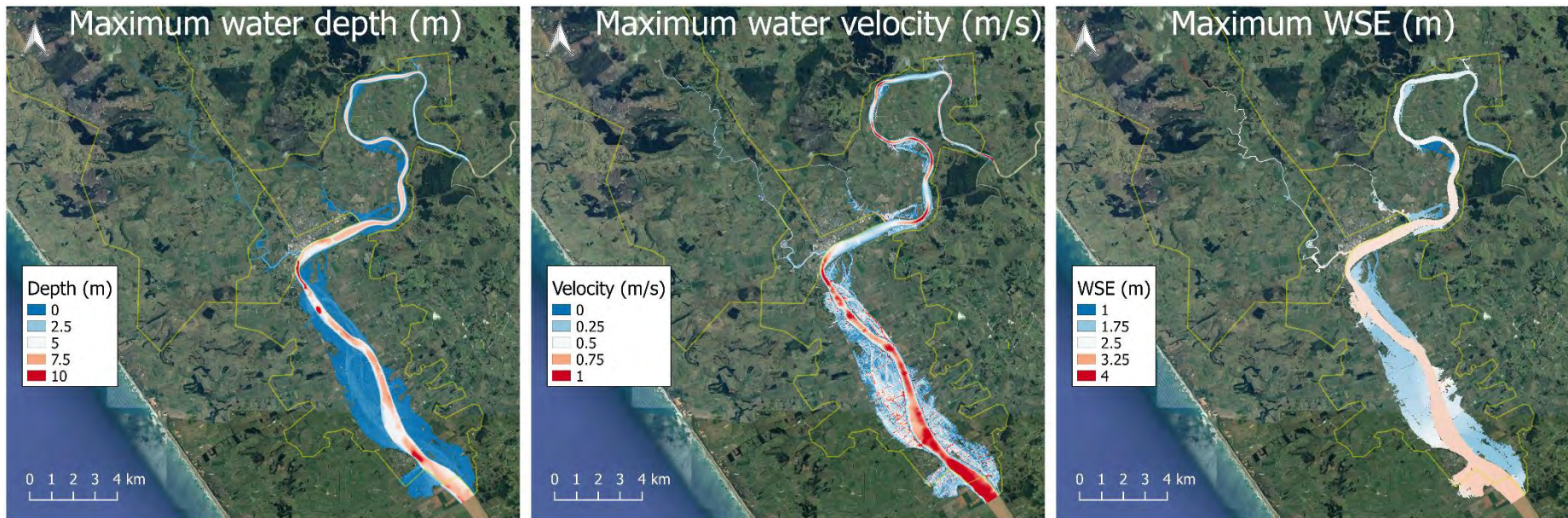


Figure 14. Kaihu – Dargaville CFHZ0 model run maximum depth, velocity and water surface elevation. Yellow line shows hazard assessment zones.

Kaihu – Dargaville CFHZ1

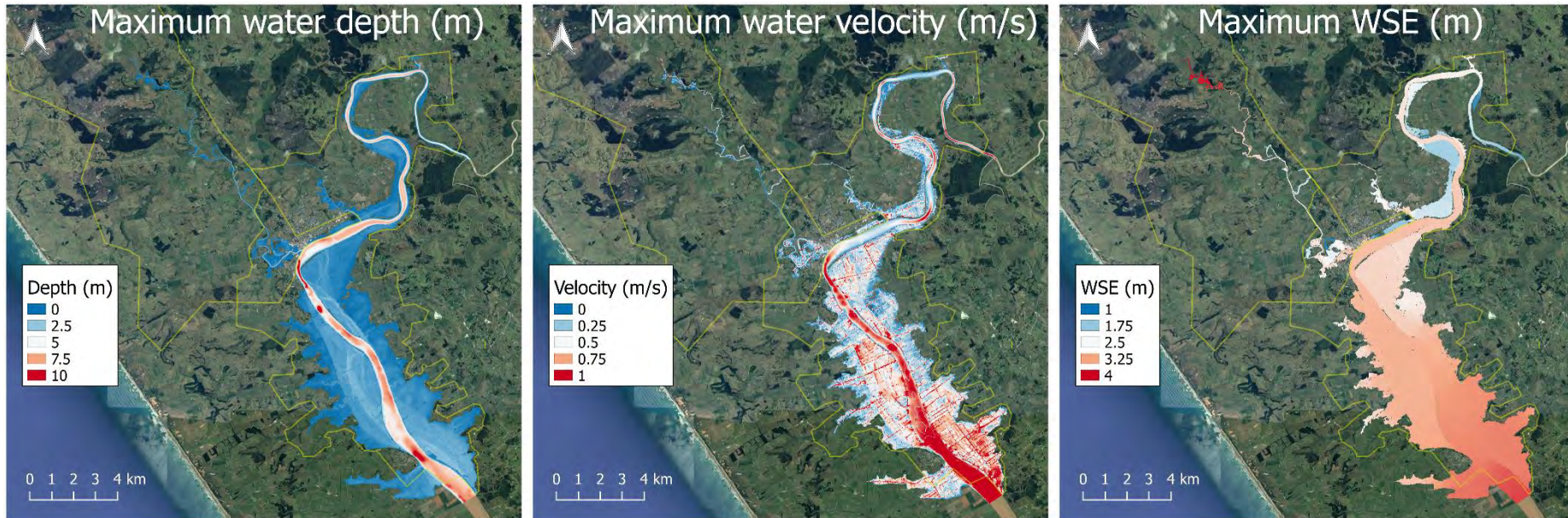


Figure 15. Kaihu – Dargaville CFHZ1 model run maximum depth, velocity and water surface elevation. Yellow line shows hazard assessment zones.

Kaihu – Dargaville CFHZ2

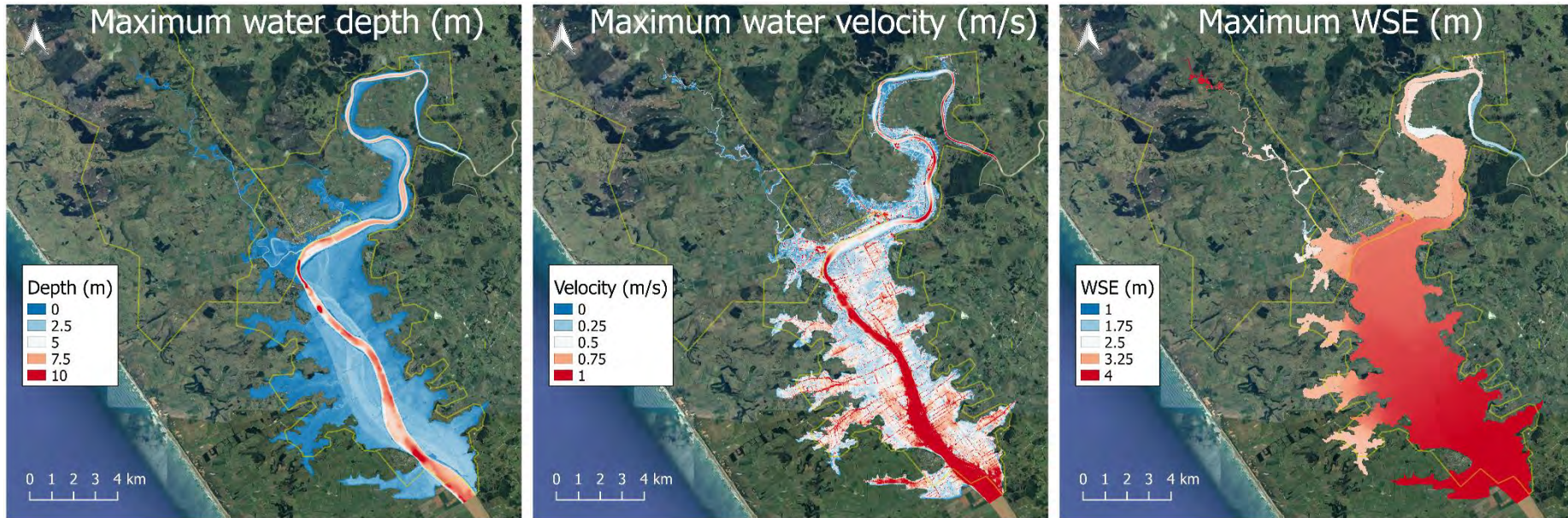


Figure 16. Kaihu – Dargaville CFHZ2 model run maximum depth, velocity and water surface elevation. Yellow line shows hazard assessment zones.

Awanui validation

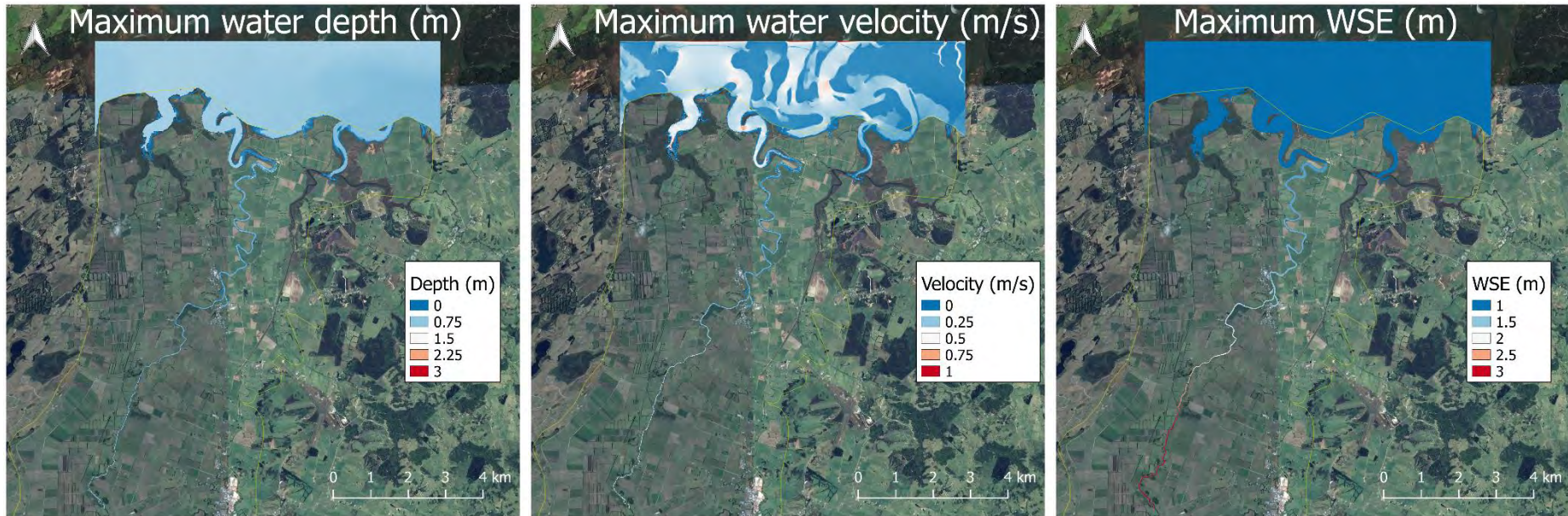


Figure 17. Awanui validation model run maximum depth, velocity and water surface elevation. Yellow line shows hazard assessment zones.

Awanui CFHZ0

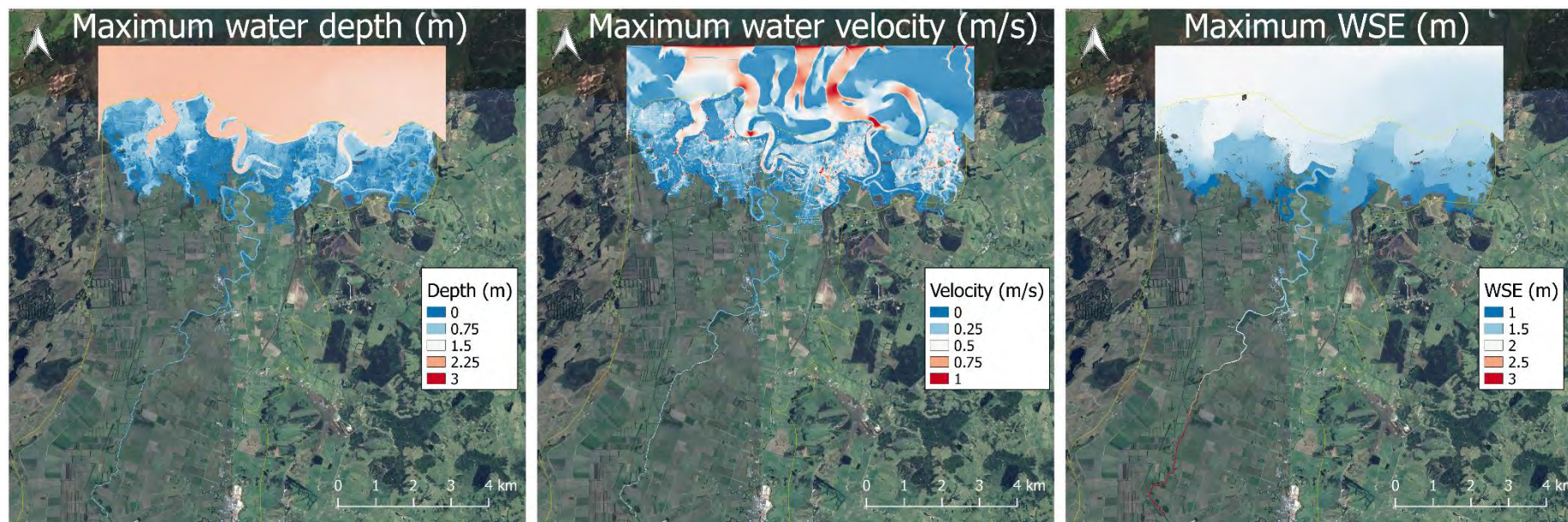


Figure 18. Awanui CFHZ0 model run maximum depth, velocity and water surface elevation. Yellow line shows hazard assessment zones.

Awanui CFHZ1

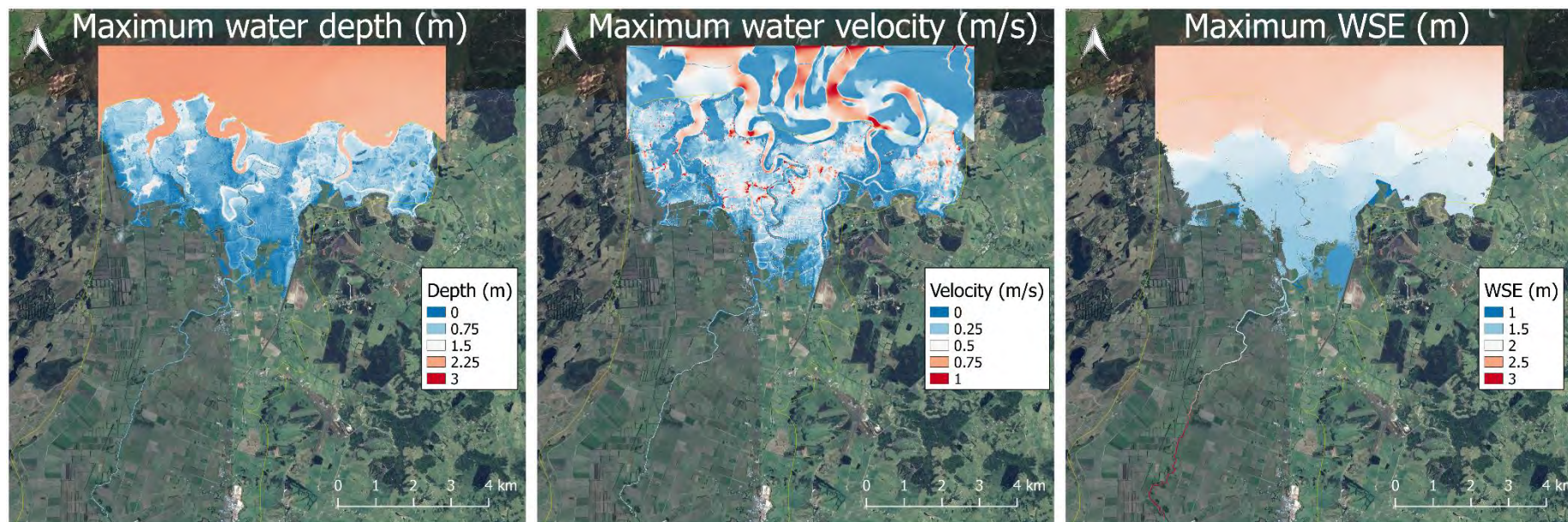


Figure 19. Awanui CFHZ1 model run maximum depth, velocity and water surface elevation. Yellow line shows hazard assessment zones.

Awanui CFHZ2

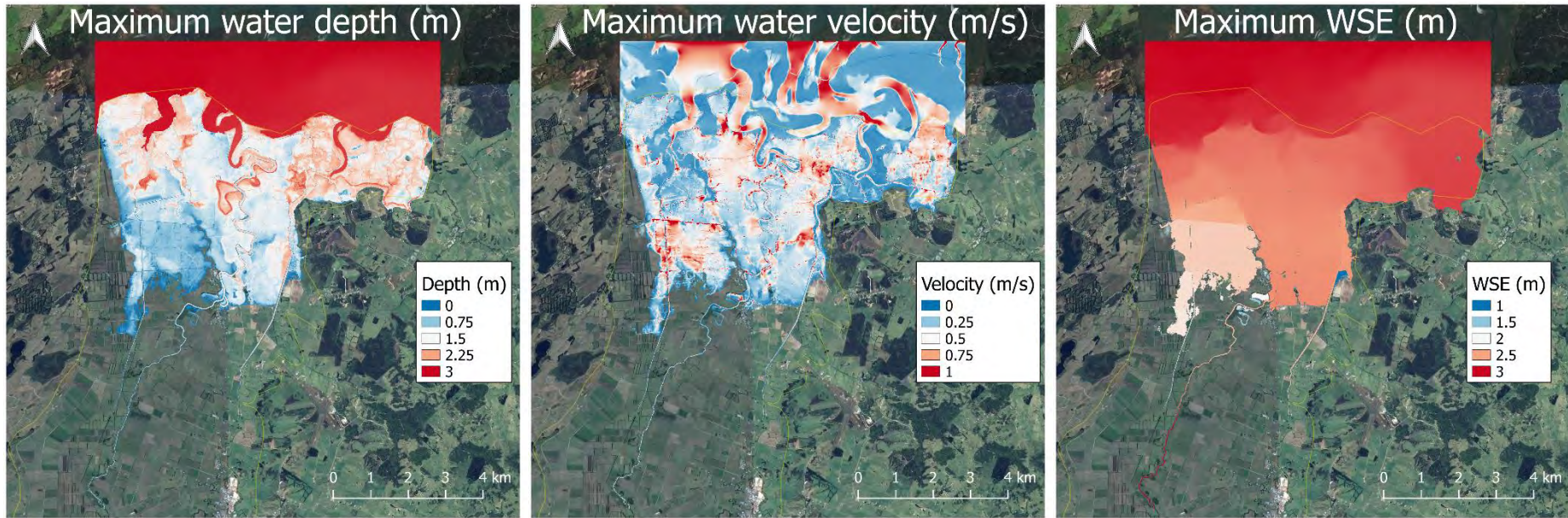


Figure 20. Awanui CFHZ2 model run maximum depth, velocity and water surface elevation. Yellow line shows hazard assessment zones.

Appendix B. CFHZ Boundary Conditions

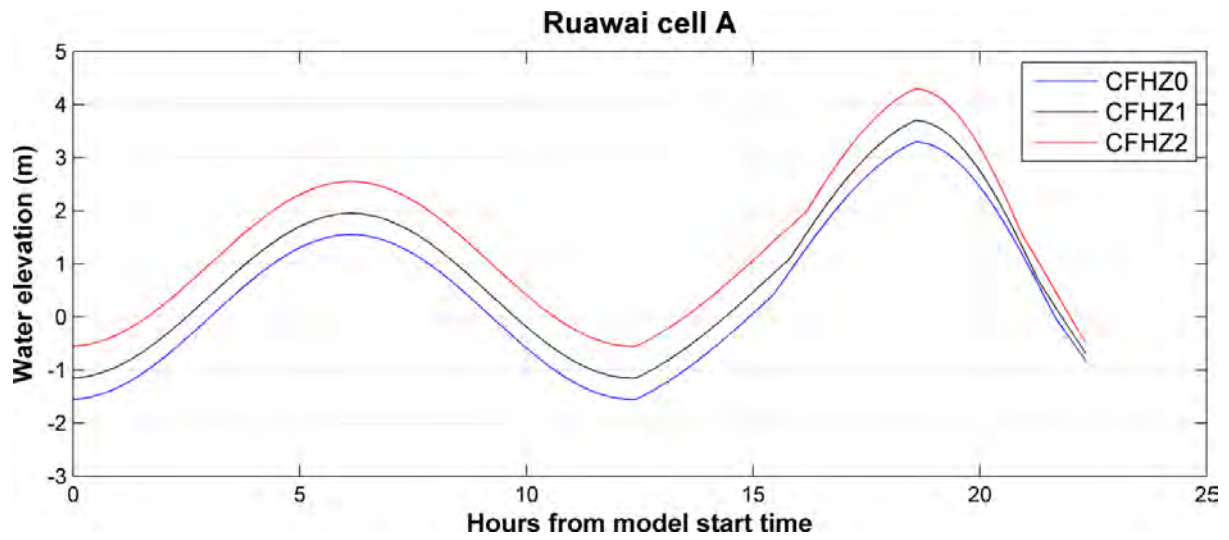


Figure 21. Estuary boundary condition time series for Ruawai cell A model runs.

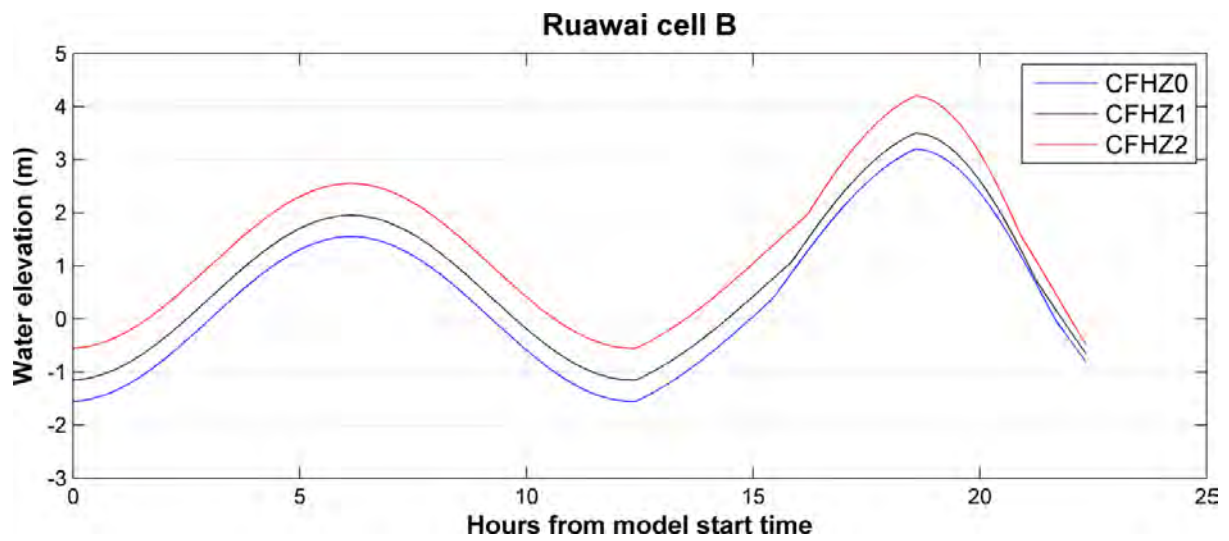


Figure 22. Estuary boundary condition time series for Ruawai cell B model runs.

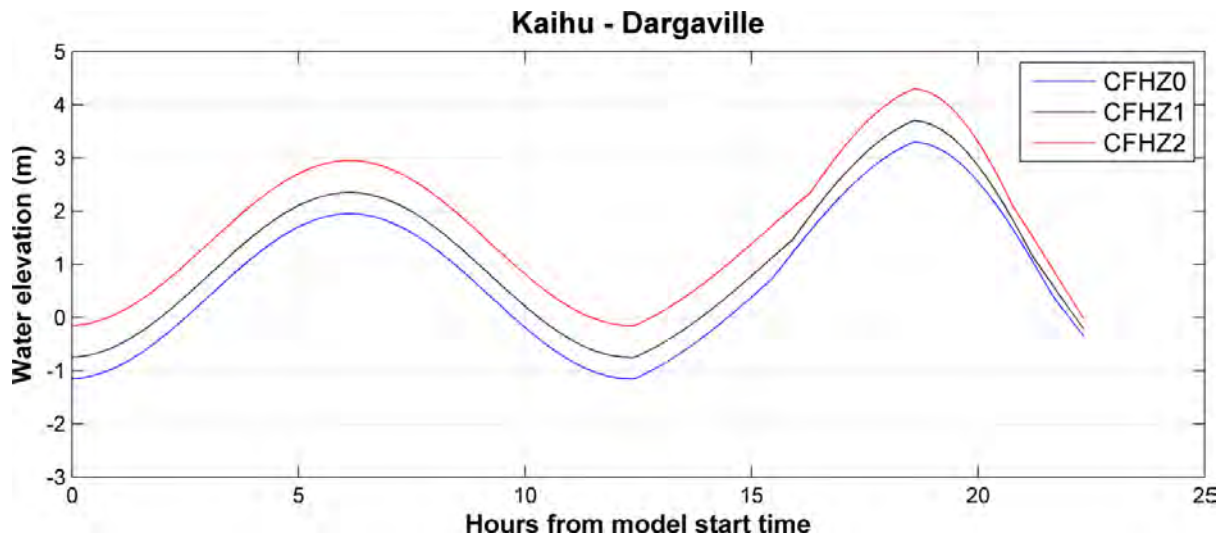


Figure 23. Estuary boundary condition time series for Kaihu - Dargaville model runs.

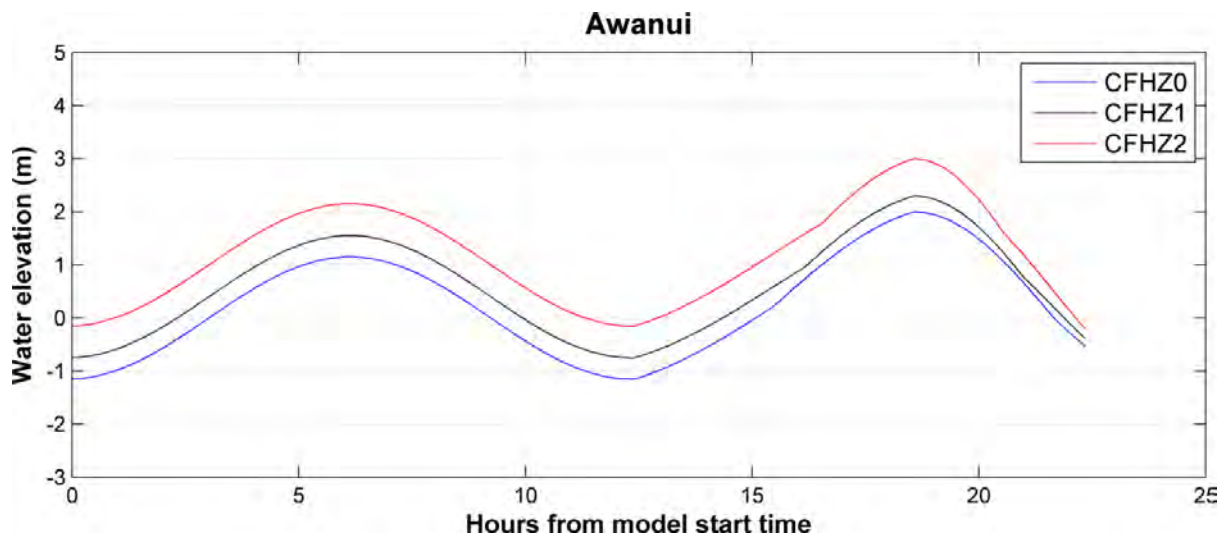


Figure 24. Estuary boundary condition time series for Awanui model runs.

Appendix C. waterRIDE

WaterRIDE™ FLOOD Manager – HEC-RAS Incorporation

WaterRIDE™ FLOOD Manager is a purpose-built floodplain management support system. Based on the waterRIDE™ time varying GIS environment, it supports the results of 1D or 2D flood models, including HEC-RAS. WaterRIDE™ FLOOD Manager is designed to enhance the understanding and communication of hydraulic modelling, as well as facilitate decision making by providing targeted flood intelligence through seamless integration of modelling results with GIS datasets.

The following instructions can be utilised to incorporate the HEC-RAS output files into NRC's WaterRIDE™ FLOOD Manager software.

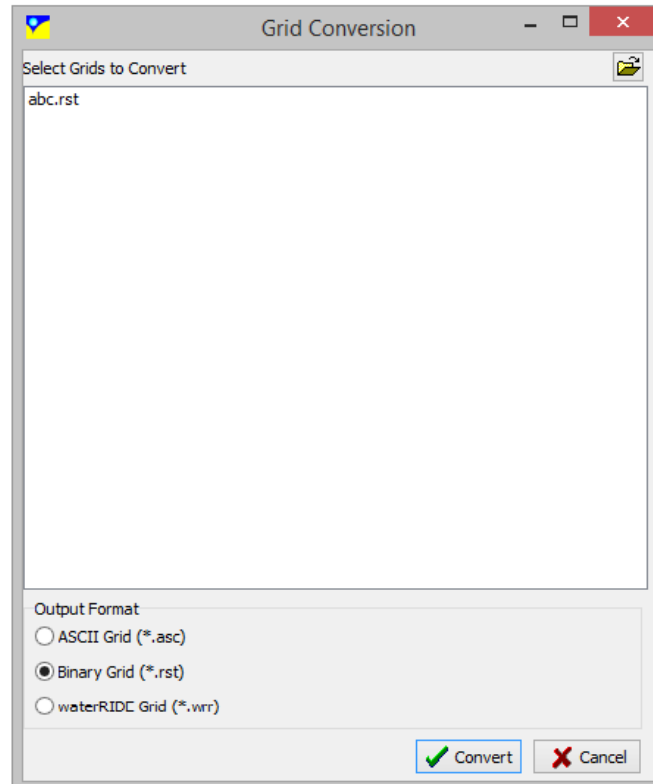
Provided files:

- Terrain GeoTIFFs (*.tif) for three model locations:
 - o 01_Ruawai\Terrain\RW.tif
 - o 02_Kaihu_Dargaville\Terrain\KD.tif
 - o 03_Awanui\Terrain\AW.tif
- Model run plan files (*.hdf) for each scenario:
 - o e.g. 01_Ruawai\Validation\Ruawai.p10.hdf
 - o e.g. 02_Kaihu_Dargaville\CFHZ0\KaihuDargaville.p20.hdf

For Viewing the HEC-RAS files in waterRIDE Flood Manager

Create a project folder and copy all of the HEC-RAS files provided (listed above). If files are moved out of this folder, WaterRIDE™ FLOOD Manager will not be able to display these files when the project is next opened.

1. Open WaterRIDE™ FLOOD Manager and start a new project from the main menu.
2. The terrain file (.tif) is converted into a waterRIDE grid (.wrr) and the 1D & 2D timeseries model results (.hdf) are converted into a waterRIDE TIN (.wrb).
3. To convert the .tif files to .wrr files in the main window navigate to Utilites > Grid Conversions, select the .tif you are wanting to convert and change the Output Format to waterRIDE Grid (*.wrr):



4. To convert the .hdf files to .wrb files in the main window navigate to Utilities > Convert 2D Model to waterRIDE. The conversion from HEC-RAS 2D results files is currently in the beta-testing phase, so if within this menu there is not an option for HEC-RAS 5, please contact David McConnell, who built the HEC-RAS 5 conversion using the 2D unsteady flow Muncie example that comes with the install:
david.mcconnell@advisian.com
+61 2 8456 7350
5. There are two modes for transferring the water surface to a DEM: **1. Mapping / Overlaying** and **2. Map-on-the-fly**.

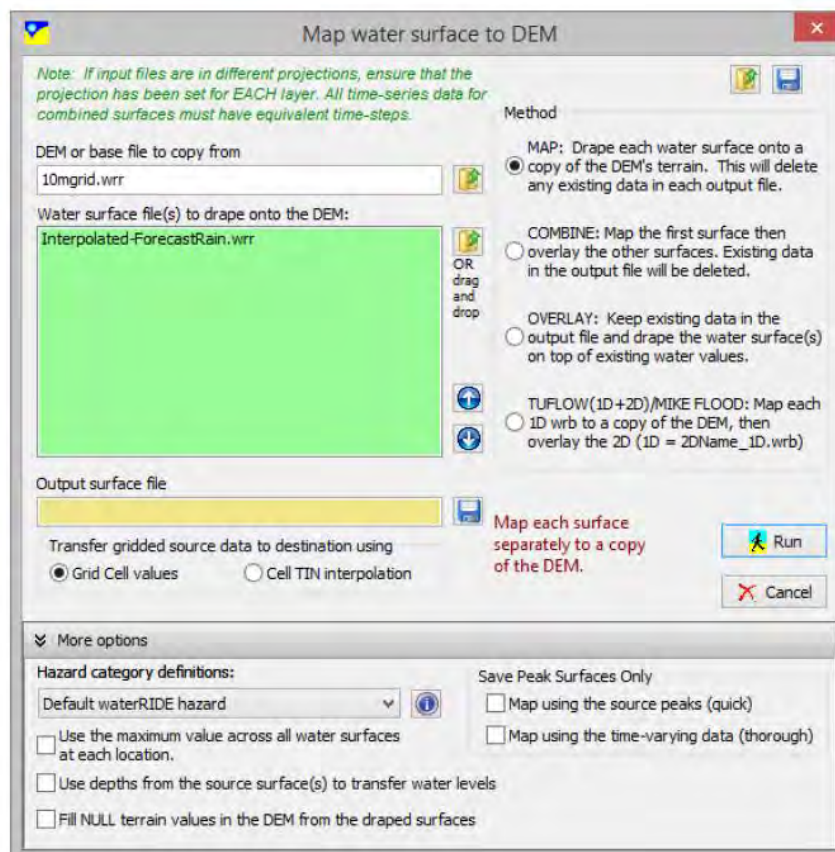
1. Mapping / Overlaying

For the mapping/overlaying operation note that grids (.wrr) and TINs (.wrb) can be interchangeably mapped to each other. To operate, select the base "DEM" file (a waterRIDE™ file containing terrain only or terrain with water - a copy of the terrain component will be extracted to a new start file), then select the water surface file(s) to map. The order can be altered in the list.

Next, select how to process the mapping:

- **Map:** Will drape each water surface into the DEM and store the outputs as *separate* files. Any non-terrain data on the base DEM will not be carried through to the output file.
- **Combine:** Will map the first file, then overlay subsequent files. The first file is mapped as standard "map" process. Information in subsequent files are overlaid onto the output file where they have valid information (non-delete value).
- **Overlay:** Initially retains any water surface information in the base "DEM" file and then sequentially overlays valid values (non-delete value) from the water surfaces.

When mapping gridded surfaces, you can specify whether the surface should be mapped as a grid (ie flat, discontinuous, terraced water surface), or as a localised TIN surface (continuous, dynamically triangulated surface between cell centroids).



2. Map-on-the-fly

Mapping a coarse TIN water surface with many timesteps to a large fine grid DEM can generate very large files. In such cases it may be more efficient in disk space (at the cost of some speed loss) to map the water surface to the DEM on the fly. The Setup Map-on-the-fly option should be used in this case, and this process creates a cross-reference index file between the TIN and the grid, and a peak properties file for rapid display of peaks. All the timeseries surfaces are mapped from the TIN to the grid as needed.